Bulletin of the Geological Society of Greece

Vol. 56, 2020

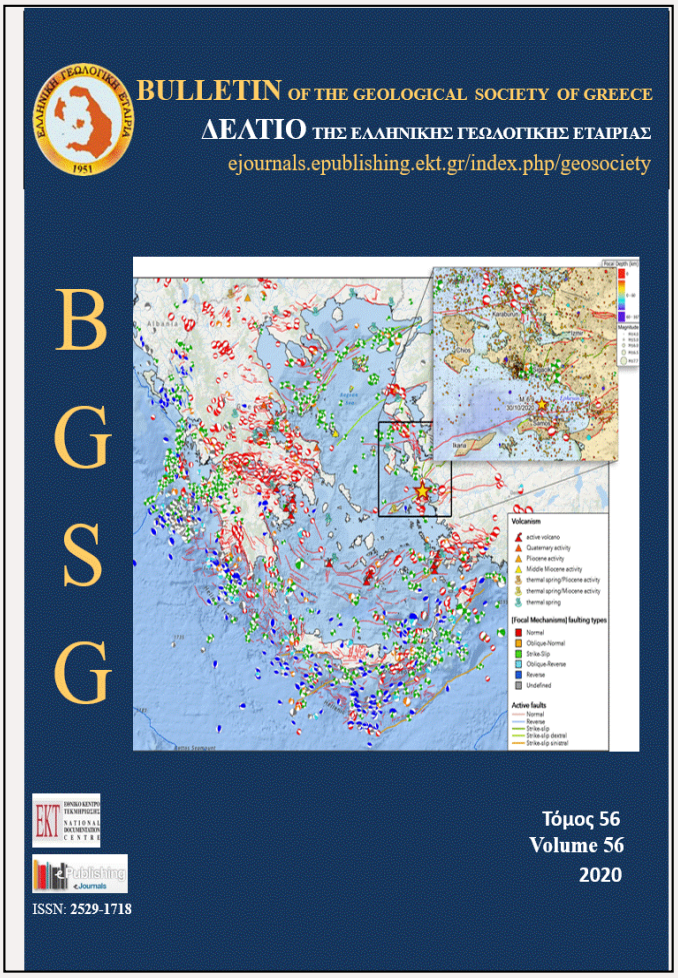

A semi-quantitative method to combine tectonic stress indicators: example from the Southern Calabrian Arc (Italy)

Scudero Salvatore — Istituto Nazionale di Geofisica e Vulcanologia, Osservatorio Nazionale Terremoti, Via di Vigna Murata 605, 00143, Rome, Italy

De Guidi Giorgio — University of Catania

Caputo Riccardo — Department of Physics & Earth Sciences, University of Ferrara, via Saragat 1, 44122 Ferrara, Italy

Perdicaro Vincenzo — Department of Biological, Geological and Environmental Sciences, University of Catania, Corso Italia 55, 95129

https://doi.org/10.12681/bgsg.23485

To cite this article:

Scudero, S., De Guidi, G., Caputo, R., & Perdicaro, V. (2020). A semi-quantitative method to combine tectonic stress indicators: example from the Southern Calabrian Arc (Italy). *Bulletin of the Geological Society of Greece, 56*(1), 280-316. doi:https://doi.org/10.12681/bgsg.23485

BGSG

Volume 56

Research Paper

Correspondence to:
Riccardo Caputo
rcaputo@unife.it

DOI number:
http://dx.doi.org/10.12681/bgsg.23485

Keywords:
Stress indicators, stress field, active tectonics, Calabrian Arc, Sicily

Citation:
Scudero S., De Guidi G., Caputo R. and Perdicaro Vincenzo (2020), A Semi-Quantitative Method To Combine Tectonic Stress Indicators: Example From The Southern Calabrian Arc (Italy). Bulletin Geological Society of Greece, 56, 280-316.

Publication History:
Received: 18/06/2020
Accepted: 28/11/2020
Accepted article online: 27/12/2020

The Editor wishes to thank two anonymous reviewers for their work with the scientific reviewing of the manuscript and Mr Ioannis Karamitros & Ms Emmanouela Konstantakopoulou for editorial assistance

A SEMI-QUANTITATIVE METHOD TO COMBINE TECTONIC STRESS INDICATORS: EXAMPLE FROM THE SOUTHERN CALABRIAN ARC (ITALY)

Salvatore Scudero[1], Giorgio De Guidi[2,3], Riccardo Caputo[4,5*]&Vincenzo Perdicaro[2]

[1]Istituto Nazionale di Geofisica e Vulcanologia, Osservatorio Nazionale Terremoti, Via di Vigna Murata 605, 00143, Rome, Italy.
salvatore.scudero@ingv.it
[2]Department of Biological, Geological and Environmental Sciences, University of Catania, Corso Italia 55, 95129. deguidi@unict.it
[3]CRUST, UR-UniCT, Catania, Italy
[4]Department of Physics & Earth Sciences, University of Ferrara, via Saragat 1, 44122 Ferrara, Italy. *rcaputo@unife.it
[5]CRUST, UR-UniFE, Ferrara, Italy

Abstract

Databases of tectonic stress indicators are commonly based on different types of observations at different spatial and temporal scales. Each single indicator can be variously representative of the real stress field and the relative importance of all the indicators should be accounted for before any following elaboration. We propose a semi-quantitative procedure which assigns weights to each indicator on the basis of its quality and its representative volume. In this way the indicators can be reliably combined to produce, for example, stress field maps or stress trajectories. The proposed weighting criterion has been applied to a dataset of 440 crustal stress indicators specifically compiled, gathering focal mechanisms and geological data from the literature, and original data from structural features derived from devoted fieldwork, for the southern part of the Calabrian Arc (Italy). This area represents an interesting case study because of its complex geodynamic and structural arrangement. Data were ranked and the orientation of the minimum horizontal stress (S_h) has been interpolated and smoothed on a regular grid. We drew maps of the principal stress axes and inferred the stress regimes over the investigated area. Results are in agreement with independent

information from the literature and display the non-uniform orientation of the tectonic stresses and the occurrence of perturbations both at regional and local scale.

***Keywords**: stress indicators; stress field; active tectonics; Calabrian Arc; Sicily.*

ΠΕΡΙΛΗΨΗ

Οι διάφορες βάσεις δεδομένων δεικτών τεκτονικών τάσεων είναι συνήθως βασισμένες σε διαφορετικούς τύπους παρατήρησης καθώς και σε διαφορετικές χωρικές και χρονικές κλίμακες. Ο καθένας από αυτούς τους δείκτες μπορεί να αντιπροσωπεύει με διαφορετικό τρόπο το πραγματικό πεδίο τάσεων και η σχετική τους αξία πρέπει να λαμβάνεται υπόψιν πριν από οποιαδήποτε τύπου επεξεργασία που επακολουθεί. Προτείνουμε μια ημι-ποσοτική διαδικασία που αποδίδει διαφορετική βαρύτητα σε κάθε δείκτη με βάση την ποιότητα του και τον ανάλογο όγκο που αντιπροσωπεύει σε δεδομένα . Με αυτόν τον τρόπο, οι δείκτες μπορούν να συνδυαστούν αξιόπιστα για να παράγουν, επί παραδείγματι, χάρτες πεδίου τάσεων ή τροχιών (διευθύνσεων) τάσεων. Το προτεινόμενο κριτήριο στάθμισης έχει εφαρμοστεί σε ένα σύνολο δεδομένων 440 δεικτών τάσεων του φλοιού που έχουν καταρτιστεί ειδικά για τον σκοπό αυτό, μέσω της συλλογής μηχανισμών γένεσης και γεωλογικών δεδομένων από τη βιβλιογραφία, καθώς και πρωτογενή δεδομένα από τεκτονικές δομές που προέρχονται από συστηματική εργασία πεδίου στο νότιο τμήμα του τόξου της Καλαβρίας (Ιταλία). Η περιοχή αυτή παρουσιάζει μεγάλο ενδιαφέρον λόγω της πολύπλοκης γεωδυναμικής και τεκτονικής της δομής. Τα δεδομένα αυτά ταξινομήθηκαν και ο προσανατολισμός της ελάχιστης οριζόντιας τάσης (Sh) έχει προσομοιωθεί στον χώρο με παρεμβολή και ακολούθως εξομάλυνση σε κάναβο. Σχεδιάσαμε χάρτες των κύριων αξόνων τάσης και εξαγάγαμε τα καθεστώτα τάσεων της περιοχής έρευνας. Τα αποτελέσματα συμφωνούν με ανεξάρτητες μεταξύ τους πηγές από τη βιβλιογραφία και αποτυπώνουν τον ανομοιόμορφο προσανατολισμό των τεκτονικών τάσεων και την εμφάνιση διαταραχών τόσο σε περιφερειακό όσο και σε τοπικό επίπεδο.

***Λέξεις-κλειδιά**: δείκτες τάσεων; πεδίο τάσεων; Ενεργός τεκτονική; Τόξο Καλαβρίας; Σικελία.*

1. INTRODUCTION

The collections of tectonic stress indicators rely on different types of data mainly derived from geological, seismological, and geodetic observations. Catalogues of indicators usually contain observations related to different temporal and spatial scales

(*e.g*. Caputo & Sato, 1996). For instance, focal mechanisms are spatially related to crustal volumes at various depths, while mesostructural data, borehole breakouts, geodetic information, and even morphological features (Nakamura, 1977) are related to much shallower crustal layers. Similarly, some of the above indicators could be representative of long geological periods (*e.g*. structural data on Quaternary deposits), or a very short time interval (*e.g*. focal solutions of instrumental earthquakes). Nevertheless, geoscientists are often inclined to combine a variety of indicators generally assuming a coherence within a broader temporal and spatial scale.

The most representative collection of tectonic stress indicators is the World Stress Map (WSM) database, started in 1986 and the last release (2018) counts more than 42,000 data records and aims to represent the present-day global stress field (Heidbach *et al*., 2018). Because of its huge data set, the WSM represents a great tool for the study of the stress pattern in various regions of the world, especially along the plate boundaries, and at different scales (see Heidbach *et al*., 2018 and references therein). The WSM catalogue considers a quality-ranking classification scheme which allows the comparability of the different stress indicators at the global scale. The classification was introduced by Zoback & Zoback (1989), and then refined and extended by Sperner *et al*. (2003) as well as Heidbach *et al*. (2010). It is internationally accepted and guarantees reliability and global comparability of the stress data. In particular, the quality classification adopted in the WSM subdivides the data into five classes according to the angular uncertainty associated to each datum. The class of decreasing quality have uncertainty within ±15°, ±15°-20°, ±20°-25°, ±25°-40°, and >±40°, respectively. Moreover, also the numerosity of the single observations which are summarized into a single indicator is taken into account in order to compare the indicators at different scales: high quality indicators result from several tens of observations, while rougher data result from only a few of observations.

The crustal stress field is mainly controlled by the plate motion, however it can be diffusely and variably controlled by second- or even third-order "genetic stress components" (Caputo, 2005) inducing stress perturbations at different scales, both in space and time. This could occur at fault tips or in correspondence of faults jogs (*e.g*. Casas *et al*., 1992; Harris, 1998; Maerten *et al*., 2002; Roberts & Michetti, 2004; Steacy *et al*., 2005; Blenkinsop, 2008), due to lateral variations of rocks' properties (*e.g*. McGarr, 1988; Caputo & Sato, 1996; Cartwright & Jackson, 2008), or sharp topographic changes (Caputo *et al*., 1985; 1988; Assameur & Mareschal, 1995). In all of those cases, an improper evaluation or weighting of the stress indicators can conceal or misinterpret the inferred stress patterns (Heidbach *et al*., 2007).

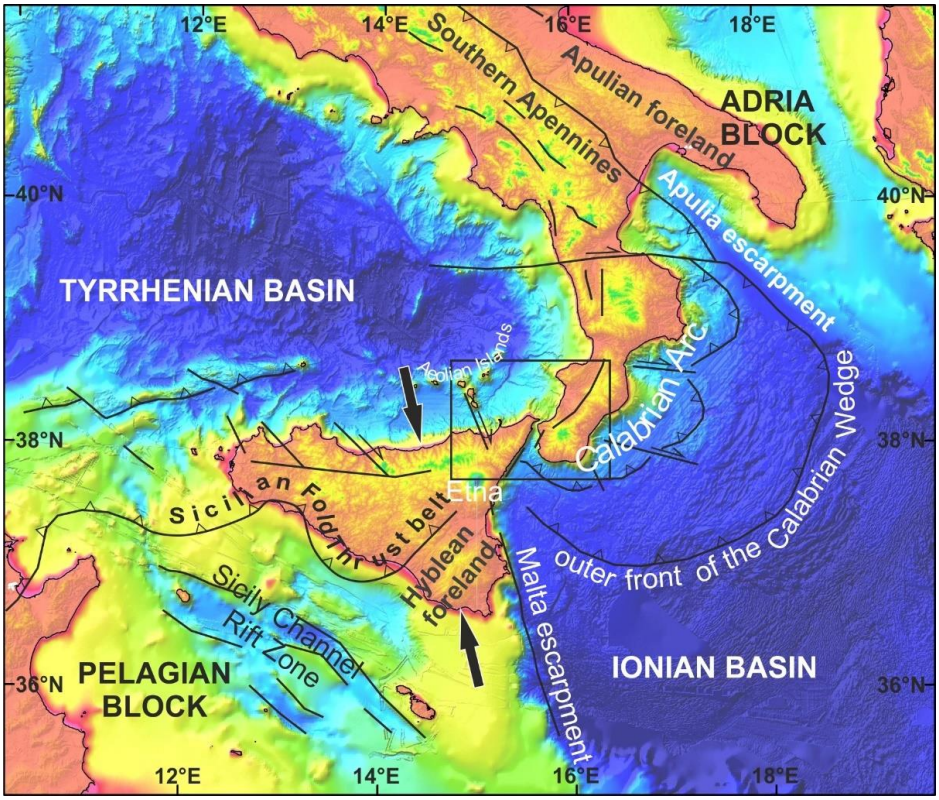

Figure 1. Geodynamic setting of the central Mediterranean area; the main lineaments are drawn after Catalano *et al.* (2008), Del Ben *et al.* (2008) and Polonia *et al.* (2011). The arrows represent the main direction of active convergence between Nubia and Eurasia plates; the box indicates the study area.

In this paper we introduce a ranking approach which is able to account for the relative differences, in terms of significance, between all the various types of stress indicators. Rather than on the numerosity, the proposed rank is based on the size of the rock volume for which each stress measure is representative of. Accordingly, by taking into account both the uncertainty of the measures, and their spatial scale, the comparison between different data would be more reliable. We firstly describe the procedure which enables an accurate evaluation of the stress indicators, then we apply the approach to a geodynamically complex region thus obtaining the trajectories of the principal horizontal stresses and, finally, we discuss the results enabling us to distinguish between different tectonic domains within the broader area, and assess multi-scale variations of the tectonic stress field.

2. METHODOLOGY

Not all the stress indicators can be considered equally reliable and representative of the real stress field; additionally, not all stress indicators have the same meaning in terms of affected rock volume. For these reasons we introduce a relative weighting criterion of the indicators on the basis of a matrix which combines a Quality Index (I_Q) with a Volume Index (I_V).

The I_Q is set as a function of the uncertainty in the stress axes determination from the meso-structural analysis or in the focal mechanism estimate. The I_Q combines the quality criteria proposed by Neri *et al*. (2005) (*i.e*. two classes at ±0°-15° and ±15°-20) and by the World Stress Map project (as described above). For the structural data the I_Q is related to the standard deviation associated to the number of structures measured at each site. On the other hand, for the focal mechanisms, a quality ranking depends on the number and quality of available seismic recordings, the number and distribution of the stations used to calculate the focal mechanism, as well as the applied inversion methodology, and the velocity model used for the inversion. For focal mechanisms, a measure of its quality is always associated and the quality factor I_Q can be retrieved straightforwardly.

In order to summarize and combine different types of data and sources, we define three qualitative classes for the I_Q, namely “low”, “medium”, and “high”. The definition criteria for seismological and geological observations are summarized in the Table 1. Moreover, we define I_V as an estimator of the volume of rock associated with each stress indicator and reasonably affected by a uniform stress field. For the structural data I_V is proportional to the volume of the outcrop where the features were surveyed, while for the focal mechanisms I_V depends on the earthquake magnitude, since the latter could be directly related to the dimensions of the rupture area and consequently to the size of the rock volume containing the reactivated fault (Kanamori & Anderson, 1975). We define three classes of I_V, namely $<10^3$ m^3, 10^3-10^6 m^3, and $>10^6$ m^3, either for seismological and geological observations, which are summarized in the Table 2.

Finally, the classes of I_Q and I_V are combined to form the matrix represented in Table 3. To the nine possible combinations are assigned five different values following a geometric progression. From Table 3 it clearly comes out that the best ranked indicators will be 16 times more influential than the rougher ones. With this semi-quantitative procedure, values of relative weight can be assigned to all indicators of a given catalogue.

Table 1. Quality Index (I_Q) and the assigned values for the focal mechanisms and structural data; s.d. stands for standard deviation.

I_Q	Focal mechanisms	Structural data	Assigned value
Low	s.d. strike ≥20°	n <10	**0.25**
Medium	10°<s.d strike <20°	n ≥10	**0.5**
High	s.d strike ≤ 10°	n ≥25	**1**

Table 2. Volume Index (I_V) and the assigned values for the focal mechanisms and structural data.

I_V		Focal mechanisms	Structural data	Assigned Value
$<10^3$ m^3	Low	M≤2	-	**0.25**
10^3-10^6 m^3	Medium	2<M<4	mesostructures	**0.5**
$>10^6$ m^3	High	M≥4	main faults	**1**

Table 3. Matrix of the weights assigned after the combination of I_Q and I_V.

		I_V		
		L	M	H
I_Q	L	2^{-4}	2^{-3}	2^{-2}
	M	2^{-3}	2^{-2}	2^{-1}
	H	2^{-2}	2^{-1}	2^{0}

3. CASE STUDY

As a case study, we applied the described methodology to purposely compiled catalogue of stress indicators for a portion of the Central Mediterranean domain corresponding to the Southern Calabrian Arc. This region is a puzzle of micro-plates where different tectonic regimes coexist in a very restricted area (Fig. 1). In particular, the Calabrian Arc is the area characterized by the greatest strain rate in the whole Italian peninsula

(*e.g*. Palano, 2015) and several strong (M>7) earthquakes affected the area in historic times (Catalano *et al*., 2008). Several recent studies have pointed out how the tectonic stress field affecting this area is highly variable (Catalano *et al*., 2008; Montone *et al*., 2012; De Guidi *et al*., 2013a; Palano *et al*., 2015; Barreca *et al*., 2019, Neri *et al*., 2020) and the causes likely lie in the interaction between large scale geodynamic processes with the regional and local tectonic ones (Pierdominici & Heidback, 2012; Soumaya *et al*., 2015). Shallow and deep variations of the crustal tectonic regime are bounded by first order crustal discontinuities which separate and accommodate different deformation patterns (De Guidi *et al*., 2013a; Presti *et al*., 2013; Scarfì *et al*., 2016; 2018).

In the Calabrian Arc, heterogeneous tectonic processes such as orogenic accretion, subduction of a narrow slab, back-arc extension, regional uplift, basaltic magmatism, and intraorogenic extension coexist shortly spaced in contiguous areas and possibly interact (Larroque *et al*., 1987; Mercier *et al*., 1992; Zoback, 1992; Vigneresse *et al*., 1999; Fabbri & Fournier, 1999; Nüchter & Stöckhert, 2008). As a consequence, heterogeneous rheological behaviours and local stress axes reorientation are likely to occur. For all these reasons, we consider the Calabrian Arc a suitable and interesting case study to apply the proposed approach.

3.1. The Catalogue

The compiled catalogue contains 440 among published and novel stress indicators, obtained from the inversion of structural and seismological data (Appendix A). All indicators fall within the area that extends from 14.8° to 16.3°E and from 37.8° to 38.7°N (Fig. 2).

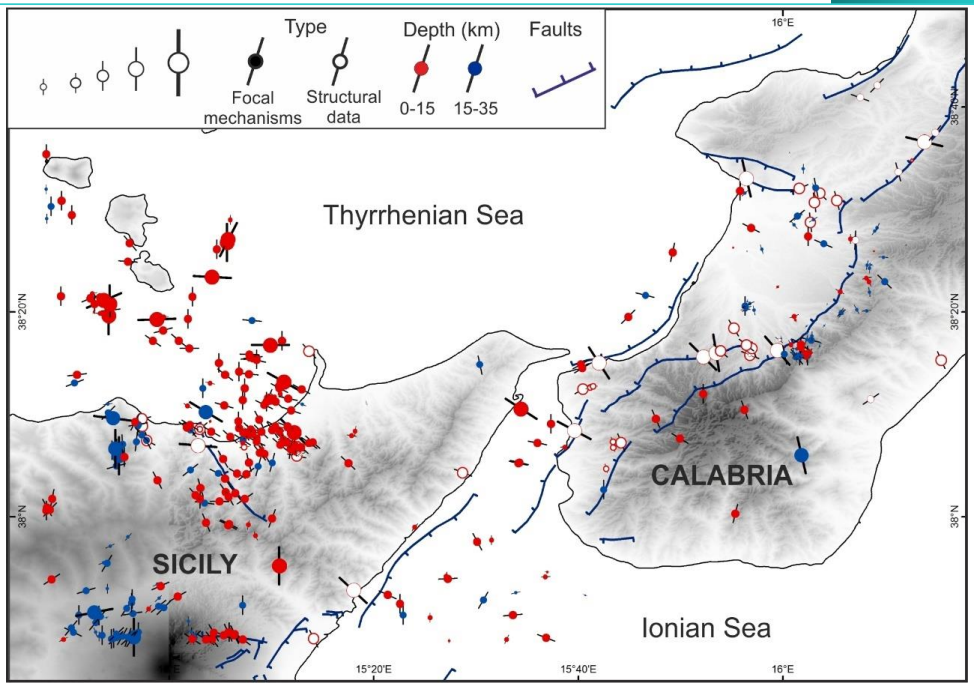

Figure 2. Map of the stress indicators collected within the study area. See inset legend for details on weight, data types, and depth of the minimum horizontal stress (S_h) indicators. The main tectonic lineaments are also shown.

The structural dataset includes published (Ghisetti, 1979a, 1979b; Tortorici *et al*., 1995; Ferranti *et al*., 2008, De Guidi *et al*., 2013a) and unpublished information relative to Quaternary outcrop scale and regional scale structural features (Fig. 2). In particular, we carried out detailed field surveys in order to collect new data where no such information was available. At this regard we measured about 1,400 meso-scale structural features at 39 different sites following the guidelines from De Guidi *et al*., 2013a; the collected data are listed in Table 4. In particular, all the surveyed sites are located on Quaternary deposits and the associated outcrops extend between 10^3 and 10^6 m^3, therefore being representative of sufficiently large rock volumes for typical mesostructural analyses (*e.g*. Mercier, 1976; Mercier *et al*., 1992; Caputo & Pavlides, 1993). The surveyed deposits mainly consist of calcarenite or other cemented sediments, avoiding not-cemented and loose matrix-supported clastic sediments where the deformation is generally accommodated in a distributed way through the relative motion between the single particles (Caputo, 2005). In the selection of the sites, we also took into account the possibility to clearly observe the geometric relationships among differently oriented structural features. For this reason, we preferred curvilinear road cuts or cliffs, wide coastal erosional surfaces and quarries enabling a 3D perspective.

For each of the 39 investigated sites (Table 4) the collected mesostructural information have been inverted with well-known numerical techniques (Caputo & Caputo, 1989; Allmendinger *et al*., 2013) to obtain the associated strain tensor and the causative stress axes by assuming coaxiality among the two tensors.

The rest of the catalogue (Appendix A) consists of 380 crustal focal solutions (<35 km) selected from published papers (Neri *et al*., 2005, Billi *et al*., 2006, Giampiccolo *et al*., 2008, Falà, 2011, Presti *et al*., 2013, De Guidi *et al*., 2013a, Scarfì *et al*., 2013). In case of earthquakes with multiple focal solutions, we choose the one with higher quality (according to the details provided by the authors), while for the events with equal ranking an average orientation has been considered. The information provided by the different authors has been parametrically homogenized by calculating the directions of T, P and B axes.

After the assignation of the weights as described in the previous section (Table 3), the catalogue contains 43 (9.8%), 98 (22.3%), and 299 (68%) indicators classified as low, medium, and high I_Q, respectively. Concerning the I_V the catalogue contains 101 (23%), 310 (70.5%), and 29 (6.6%) indicators pertaining to low, medium, and high I_V, respectively. After the combination of the two indexes, we obtained the following distribution of combined weights: 28 (6.4 %) indicators with the maximum possible normalised weight of "1", 224 (50.9 %) indicators with weight "0.5", 116 (26.4%) indicators with weight "0.25", 48 (10.9 %) indicators with weight "0.125", and 24 (5.5 %) indicators with the lowest assigned weight of "0.0625".

Moreover, on the base of the hypocentral distribution of the earthquakes, showing a sharp decrease at ca. 15 km, probably due to a rheological variation which has also been highlighted by a local crustal tomography (Presti *et al*., 2013). Accordingly, we split the database into two datasets, respectively above and below the 15 km-depth. The catalogue lists 204 indicators (54.3%) pertaining to the shallower crust and 172 indicators (45.7%) pertaining to the deeper one.

The ranked catalogue is then exploited to reconstruct the horizontal stress field of the investigated area for the two crustal layers. The differences in the azimuthal distribution of T, P, and B axes, with and without the assignation of the weights, show a similar general trend (Fig. 3) which is equivalent to the 1st-order stress of the area. However, the two distributions show some different second-order features (*i.e.* relative minimum/maximum). The weighted data were interpolated on a regular grid using the software proposed by Carafa *et al*. (2015) and available online (http://shine.rm.ingv.it/),

it adopts the algorithm proposed by Bird & Li (1996) and updated by Carafa & Barba (2013). Taking into account the data distribution, their density, and the scale of our analysis, the search radius for the interpolation was fixed at 24 km, so that areas not covered by data are not interpolated. This value derives from a trade-off between the density of data and the desired resolution and it is greater than the boundary of data split (*i.e.* 15 km). In general, brittle deformation which occurs in the uppermost crust is considered more discontinuous than the deformation in deeper parts, therefore the two sub-sets of data can be considered as totally independent because of i) the different rheological behaviour and deformation mechanisms of the two crustal layers; ii) the causes of the variations of the spatial are usually 2D features with high aspect ratio (De Guidi *et al*., 2013a). As above mentioned, data have been statistically weighted based on their combined quality indexes.

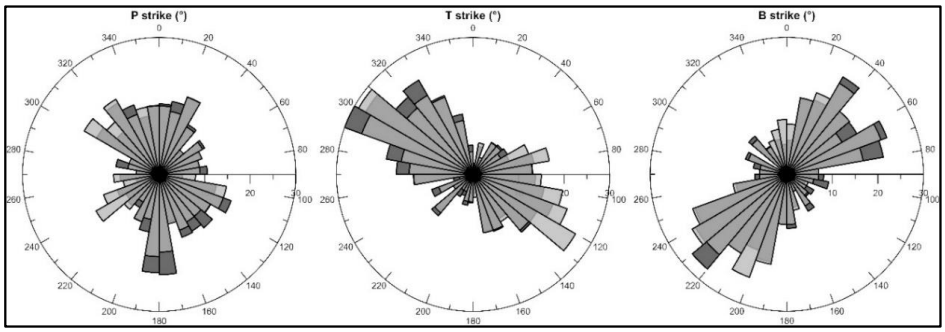

Figure 3: Relative azimuthal distribution of the T, P, and B axes before (light grey) and after (dark grey) the weighting; bin size = 10°.

We reconstructed three distinct maps by separately interpolating the three principal stresses based on their horizontal projection. From the analyses we excluded those with plunge >20° because more plunging angles could bias the results (Fig.4).

Table 4. Stress indicators after meso-structural fieldworks. Type: F = indicators from main fault planes; J = set of extensional joints. The weight W of each indicator is calculated from I_Q and I_V as explained in the text.

Type	Lat_N	Long_E	P_strike	P_plunge	T_strike	T_plunge	B_strike	B_plunge	I_q	I_V	W
J	37,80	15,24	266	87	154	1	64	3	H	M	0.5
J	38,07	15,48	207	79	112	1	21	11	H	M	0.5
J	38,08	15,71	313	76	167	12	75	8	M	M	0.25
F	38,10	15,21	101	65	282	25	192	0	L	M	0.125
J	38,10	15,21	7	56	102	4	195	34	H	M	0.5
F	38,10	15,21	113	74	291	16	21	1	L	M	0.125

F	38,10	15,21	156	63	341	27	250	2	M	M	0.25
F	38,10	15,21	164	77	309	11	41	7	L	M	0.125
F	38,10	15,08	282	11	13	3	120	79	L	M	0.125
F	38,10	15,21	306	67	127	23	37	0	L	M	0.125
F	38,10	15,21	108	78	278	12	9	2	L	M	0.125
J	38,11	15,72	352	84	157	6	247	2	M	M	0.25
J	38,11	15,12	169	46	264	4	358	44	M	M	0.25
F	38,11	15,21	317	57	134	33	225	2	L	M	0.125
J	38,12	15,21	26	23	294	5	192	67	M	M	0.25
F	38,12	15,21	285	73	108	17	18	1	M	M	0.25
J	38,12	15,74	100	86	338	2	248	3	H	M	0.5
J	38,12	15,72	42	76	161	7	253	12	M	M	0.25
J	38,12	14,96	30	79	299	0	209	11	H	M	0.5
J	38,13	15,18	233	75	347	6	78	13	M	M	0.25
F	38,13	15,18	104	83	265	7	355	2	M	M	0.25
J	38,14	15,05	185	89	49	1	319	1	H	M	0.5
J	38,14	15,05	0	0	319	1	0	0	H	L	0.25
J	38,15	14,96	72	68	336	2	245	22	H	M	0.5
J	38,16	14,96	108	77	258	11	349	6	H	M	0.5
F	38,19	15,32	70	63	245	27	340	0	L	M	0.125
F	38,19	16,14	60	72	236	18	326	1	H	M	0.5
J	38,21	15,67	252	85	60	5	150	1	H	M	0.5
J	38,21	15,69	243	87	70	3	340	0	M	M	0.25
J	38,21	15,69	342	78	90	4	181	11	M	M	0.25
J	38,25	16,26	88	83	336	3	246	6	H	M	0.5
J	38,26	15,95	216	85	112	1	22	5	H	M	0.5
F	38,26	15,95	116	82	296	8	206	0	M	M	0.25
F	38,27	15,89	140	76	351	12	263	8	H	H	1
J	38,27	15,23	190	84	317	4	47	5	H	M	0.5
J	38,27	15,90	321	85	132	5	222	1	H	M	0.5
J	38,27	15,95	234	87	332	0	62	3	H	M	0.5
J	38,28	15,94	184	88	309	1	39	2	H	M	0.5
F	38,29	15,99	143	87	307	2	37	1	M	M	0.25
J	38,31	15,92	146	87	329	3	239	0	H	M	0.5
F	38,45	16,12	273	53	94	36	3	1	H	M	0.5
J	38,48	16,04	265	48	174	1	84	42	H	M	0.5
J	38,51	16,05	245	71	76	19	345	3	M	M	0.25
J	38,51	16,05	289	62	77	25	173	13	H	M	0.5
J	38,51	16,09	345	89	166	1	76	0	H	M	0.5
J	38,53	16,06	329	87	133	3	223	1	H	M	0.5
J	38,53	16,03	185	88	67	1	337	2	H	M	0.5
F	38,56	16,19	26	86	165	3	255	2	H	M	0.5
F	38,62	16,25	261	77	38	8	123	9	H	M	0.5
F	38,68	16,13	124	78	290	11	20	3	H	M	0.5
F	38,70	16,15	296	83	44	2	134	7	H	M	0.5

3.2. Results

The average direction of the minimum horizontal stress (S_h) is N121° and it is in good agreement with the regional extensional direction in the Late Pleistocene time as established in the literature (Monaco *et al*., 1997; Catalano *et al*., 2010; Billi *et al*., 2007), and also the overall superficial pattern observed in the area is the same observed by GNSS inversions (D'Agostino & Selvaggi, 2004; Palano *et al*., 2015). Results also nicely match with the geometric and kinematic parameters of the main Quaternary faults affecting the area (Fig.2). On the other hand, for the deeper layer the stress trajectories of all the three principal axes show the existence of different sub-subdomains which are characterized by variable orientations (Fig.4).

As a first approximation, assuming an Andersonian stress field and considering that the two principal horizontal stresses must be mutually orthogonal, we juxtaposed the three maps (one for each principal stress) in order to verify the areas where orthogonality occurs and among which couple of axes this occurs (Fig. 5). For the shallower layer (0-15 km) this assumption is verified in most of the study area, however in some sectors (Capo Vaticano promontory and southern Ionian Calabria and its offshore) none of the three possible couples of horizontal principal stress axes is orthogonal (Fig. 5). The lack of this condition could be due to the similarity, in magnitude, among the three principal axes and therefore the tectonic stress regime is likely represented by a cylindrical stress tensor and the corresponding ellipsoid has a revolution symmetry around a vertical σ_1 axis.

Following the above reasoning, we could thus identify and distinguish different Andersonian regimes characterizing the investigated region (Fig. 6). The obtained results highlight a transcurrent regime in the northern offshore of Sicily and Aeolian Islands (green area in Fig. 6): the projections of σ_1 and σ_3 are therefore orthogonally arranged and their orientation is coherent with the NW-SE dextral transcurrent kinematics recognized in the area (Fig.5; Palano *et al*., 2012; 2013b; Gallais *et al*., 2013; Barreca *et al*., 2019).

A compressive tectonic regime (blue area in Fig. 6) with the projections of σ_1 and σ_2 orthogonally arranged characterizes the SW corner of the study area. The regime, and its orientation is coherent with the compressional belt recognized in Sicily west of Mount Etna and related to the activity of a regional basal thrust (Fig 4; Lavecchia *et al*., 2007; De Guidi *et al*., 2015).

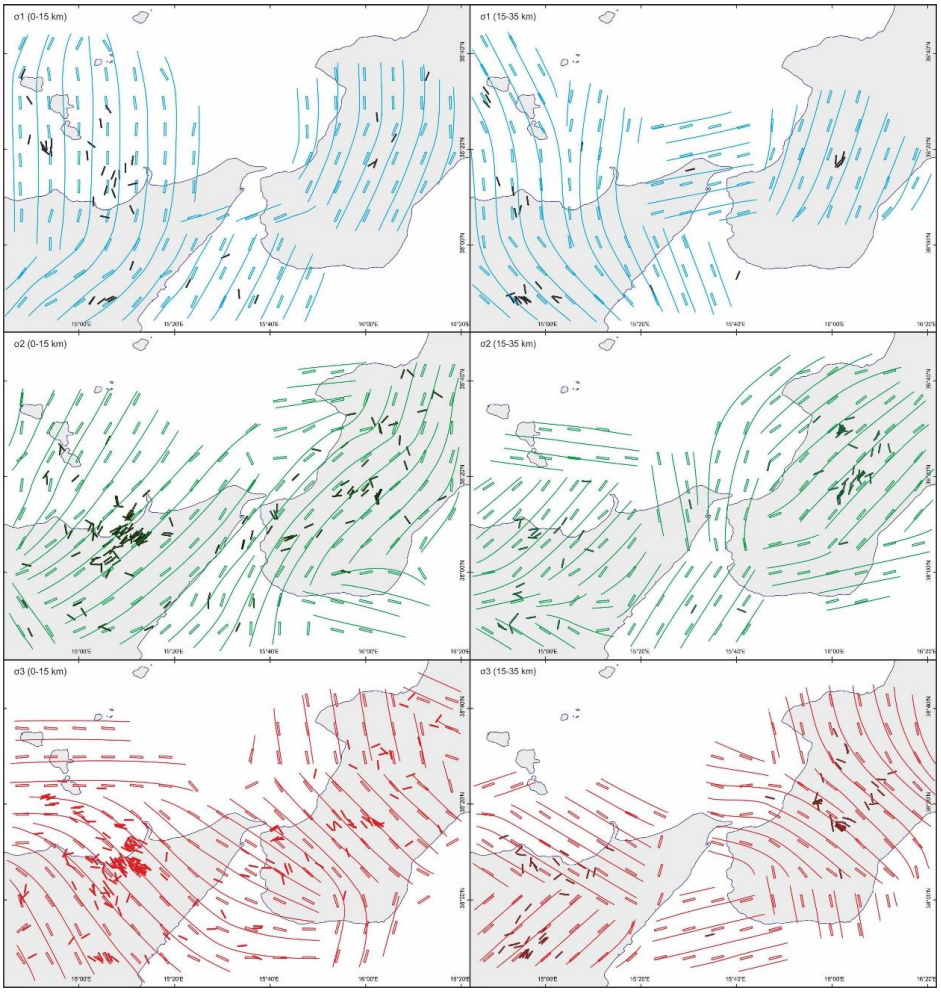

Figure 4: Inferred smoothed stress trajectories of the three principal axes based on the horizontally projected data with plunge <20°, interpolated using the software SHINE (Carafa *et al.*, 2015). Maps in the left and right columns represent the shallow (0-15 km) and deeper layers (15-35 km), respectively.

Most of the study area is instead characterized by an extensional regime (yellow area in Fig. 6), in which σ_1 is vertically oriented and the σ_2 and σ_3 lie on the horizontal plane. The main trend of the trajectories, with the least axis (red lines) varying from E-W to NW-SE (Fig. 5), represents the first-order regional stress field (De Guidi *et al*., 2013a) and it is in agreement with the main tectonic structures of the area (Catalano *et al*., 2008).

Finally, the Capo Vaticano promontory and the southern Ionian Calabria and its offshore, are also characterized by a broadly tensile tectonic regime where the

magnitude of the two horizontal axes likely becomes comparable and hence the used statistical procedure is not able to picture out a well-defined Andersonian stress field with two mutually orthogonal trajectories of the principal horizontal stresses (pink areas in Fig. 6). In these sectors, the paucity of the input data could also contribute to this uncertainty. For the southern Calabria sector, this tectonic regime is in continuity with the extensional one (yellow area), and the stress trajectories of the two horizontal axes are in lateral continuity although the two horizontal axes are swapped in the two sectors (Fig. 5). Conversely for the Capo Vaticano promontory the trajectories are not coaxial with the surrounding extensional field.

The same procedure was also applied to the deeper crustal layer (15-35 km); but in this case the results show a patchy distribution of the principal stress axes (Fig.5). The conditions of distinct orthogonal stress axes and the corresponding pair of horizontal stresses are laterally limited and show frequent and sharp variations (Fig. 5 bottom). To this heterogenous stress field contributes the fact that, the Andersonian condition that one of the principal axes must be vertical (*i.e.* perpendicular to the Earth surface) is progressively vanishing at increasing depth.

4. DISCUSSION

A weighting criterion for stress indicators has been proposed and used to compute a regional-scale stress map in an area characterized by a complex tectonic arrangement (Southern Calabrian Arc). There is not a "target" model to match or that could represent an independent reference to compare the outcome of the elaboration with weighted and un-weighted data. Of course, differences arise because of the changes in the input data (Fig. 3), but the results cannot be evaluated in absolute terms. Because the distribution of the stress indicators over the investigated area is uneven, we could incur in the possible influence of any irregular and/or clustered data distribution. However, the results of the interpolation are reliable and blanks areas are left where data are not dense enough to properly interpolate the trajectories (Fig. 4). The comparison between the shallow (<15 km) and deep (15-35 km) trajectories interpolated for each principal stress axis shows several high-angle variations (even orthogonal) arrangement at the same location (Fig. 4). In the shallow crust, the S_h trajectories are generally more coherent with the regional picture (first-order field), while in the deeper crust they show marked azimuthal differences in many distinct zones.

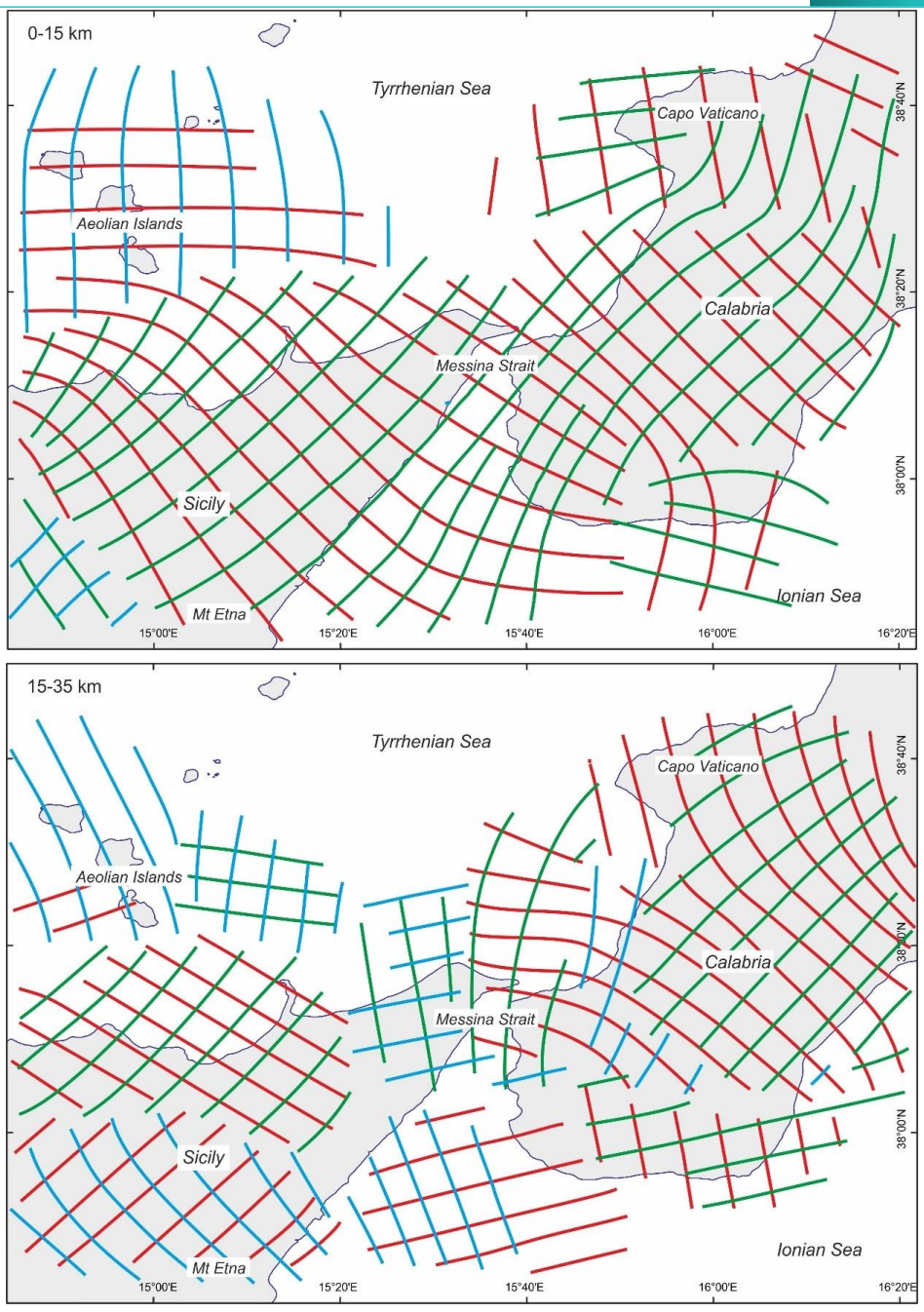

Figure 5. Areas characterized by two orthogonal horizontal (or quasi-orthogonal) principal axes for the subset of data 0-15 km (top) and 15-35 km (bottom). Blue, green, and red lines indicate the trajectories of the three principal axes: σ_1, σ_2, and σ_3 respectively.

In this context, the stress perturbations documented by De Guidi *et al*. (2013a) which have been associated with the major crustal fault segments affecting the area, should be considered as even lower order variations. Within the composite setting of the investigated area, the Messina Straits deserves some specific notes. The area is defined as a "tectonic puzzle" because of the tangle of fault segments at different scales and with different orientations which shape the Straits (Doglioni *et al*., 2012). Among these, the source of the 1908 Mw=7.1 earthquake is still debated (Aloisi *et al*., 2012, Meschis *et al*., 2019). The smaller scale variations could be recognized only with much denser and local-scale datasets, while at the broader scale of the present investigation such deflections are barely recognizable. We cannot exclude the existence of horizontal or sub-horizontal discontinuities or sharp vertical changes in the mechanical properties of the crust. In fact, large Vp anomalies in the crustal structure of the Calabrian Arc are well documented in recent tomographies (Neri *et al*., 2012; Presti *et al*., 2013; Palano *et al*.; 2015; Scarfì *et al*., 2016) and reflect the articulated crustal structures.

On the other hand, differences between the shallow and the deep layers can be straightforwardly interpreted in the frame of the broader geodynamics of the area, probably in connection with the Ionian subduction and the processes leading to the crustal thickening of the upper plate (Barreca *et al*., 2020). In particular, the compressional regime in mainland Sicily (blue area in Fig. 6), would be the result of the Nubia-Eurasia convergence and this domain is separated from the broadly extensional domain (yellow in Fig. 6) by a NW-SE boundary that is a portion of a larger transition zone highlighted by several authors and interpreted as a major separation zone between two different crustal blocks (Polonia *et al*., 2011; Palano *et al*., 2012; 2015; Gallais *et al*., 2013). Hence the reasons leading to the differences between shallow and deep layers can be various, and we have also to consider that in the deeper layer the actual stress field could be more complex and uneven with respect to the imaged picture in Figure 5, for example due to the presence of the subducting Ionian slab. Indeed, in different tectonic regimes the depth of the brittle–ductile transition generally differs (Paterson and Wong, 2005; Jaeger *et al*., 2007) being also associated to different values of the maximum strength (Maggini and Caputo, 2020), with stronger rocks in compression and weaker in tension. Further reasons for these ravelling results could be the data distribution. Indeed, in the deeper layer the exploited dataset is poorer and more scattered than in the shallow one, thus showing a higher lateral variability (Fig. 4), and several blank areas result from the interpolation. It should be also recalled that the applied procedure assumes Andersonian stress fields, which maybe not always valid at greater depths. Obviously, a combination between the above causes is also plausible.

For the above reasons, it is not possible with the available data to map the tectonic regime in the deeper layer.

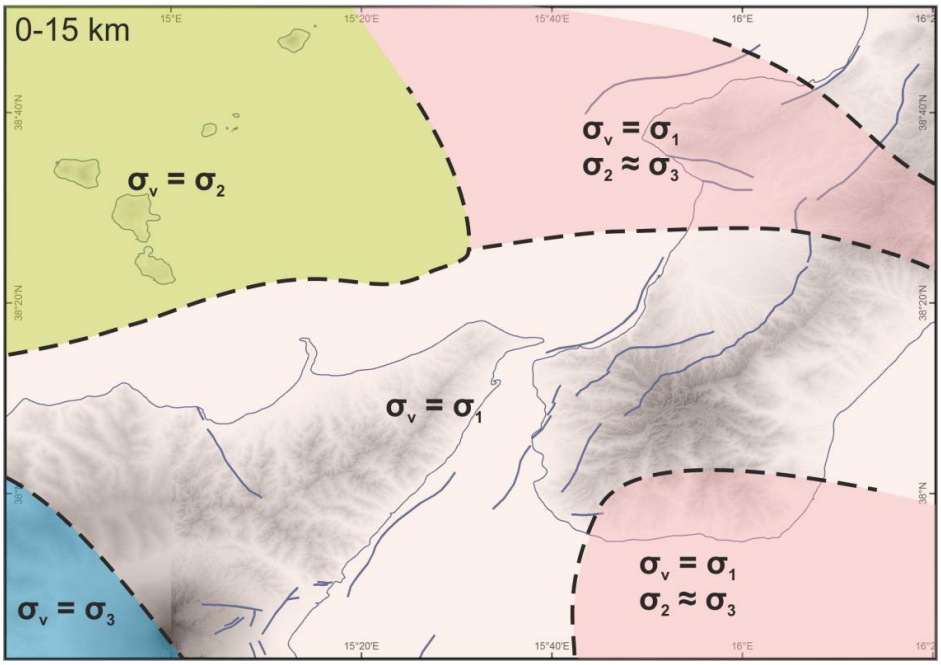

Figure 6. Sketch summarizing the inferred tectonic regimes affecting the shallow crust (0-15 km) in the investigated area.

5. CONCLUDING REMARKS

In this note, we introduced a straightforward procedure to determine the relative weight of tectonic stress indicators commonly used as input data to map the stress field at various scales. After the compilation of a catalogue of stress indicators in a region characterized by a complex pattern, we applied the proposed weighting criterion and compared the results with the literature. The computed stress trajectories are generally in good agreement with previous studies and allowed to recognize the different tectonic regimes affecting the area.

Supported by devoted fieldworks, we collected the largest available dataset of Late Pleistocene-to-present tectonic stress indicators for the southern Calabrian Arc. We have been able to investigate the tectonic stress and its spatial variations, both vertical and horizontal across the study area.

The methodology proposed in this study represents a new approach which is able to provide a relative ranking of data to account for the quality of data themselves and for the representative volume of each indicator. The application of this procedure is possible to any dataset which contains the basic information about how indicators are gathered and can be applied to investigations at different scales (*i.e*. regional and local). In particular, it could be very useful to describe areas in complex geodynamic contexts and provide consistent pictures of the stress pattern. For the present case study, the greatest limitation is due to the irregular spatial distribution of the data: a homogeneous coverage of stress indicators could indeed allow a complete 3D interpolation of stress trajectories, and stress regimes based on a narrower crustal slicing. Moreover, whether necessary, the weight matrix here proposed can be specifically calibrated according to the knowledge of a given region, or after expert judgement.

As a final comment, this approach can also indirectly address seismic hazard assessment studies, highlighting the possible reactivation on faults, or any inherited crustal discontinuity, that is favourably oriented with respect to the stress field, also suggesting its probable kinematics.

5. ACKNOWLEDGMENTS

The research was supported by PRIN 2017 Project "Overtime tectonic, dynamic and rheologic control on destructive multiple seismic events - Special Italian Faults & Earthquakes: from real 4D cases to models" (responsible G. Lavecchia).

6. REFERENCES

Allmendinger R.W., Cardozo, N.C., & Fisher, D., 2013. Structural Geology Algorithms: Vectors and Tensors. Cambridge, England, Cambridge University Press, 289 pp.

Aloisi, M., Bruno, V., Cannavò, F., Ferranti, L., Mattia, M., Monaco, C., & Palano, M., 2013. Are the source models of the M 7.1 1908 Messina Straits earthquake reliable? Insights from a novel inversion and a sensitivity analysis of levelling data. *Geophysical Journal International*, 192(3), 1025-1041, doi: 10.1093/gji/ggs062.

Assameur, D.M. & Mareschal, J.-C., 1995. Stress induced by topography and crustal density heterogeneities: implication for the seismicity of southeastern Canada. *Tectonophys*., 241, 179-192.

Barreca, G., Branca, S., Corsaro, R. A., Scarfì, L., Cannavò, F., Aloisi, M., & Faccenna, C., 2020. Slab Detachment, Mantle Flow, and Crustal Collision in Eastern Sicily (Southern Italy): Implications on Mount Etna Volcanism. *Tectonics*, 39(9), e2020TC006188.

Barreca G., Scarfì L., Gross F., Monaco C., De Guidi G., 2019. Fault pattern and seismotectonic potential at the south-western edge of the Ionian Subduction system (southern Italy): New field and geophysical constraints. *Tectonophys*., 761, 31–45, doi: 10.1016/0040-951(85)90064-2.

Billi, A., Barberi, G., Faccenna, C., Neri, G., Pepe, F., & Sulli, A., 2006. Tectonics and seismicity of the Tindari Fault System, southern Italy: crustal deformations at the transition between ongoing contractional and extensional domains located above the edge of a subducting slab. *Tectonics*, 25(2), doi: 10.1029/2004TC001763.

Billi, A., Presti, D., Faccenna, C., Neri, G., & Orecchio, B., 2007. Seismotectonics of the Nubia plate compressive margin in the south Tyrrhenian region, Italy: Clues for subduction inception. *J. Geophys. Res.: Solid Earth*, 112(B8). doi: 10.1029/2006JB004837.

Bird, P., & Li, Y., 1996. Interpolation of principal stress directions by nonparametric statistics: Global maps with confidence limits. *J. Geophys. Res.*, 101, 5435-5443.

Blenkinsop, T.G., 2008. *Relationships between faults, extension fractures and veins, and stress. J. Struct. Geol*., 30, 622-632, doi: 10.1016/j.jsg.2008.01.008.

Caputo, M. & Caputo, R., 1989. Estimate of the regional stress field using joint systems. *Bull. Geol. Soc. Greece*, 23, 101–118

Caputo, M., Manzetti, V. & Nicelli, R., 1985. Topography and its isostatic compensation as a cause of seismicity; A revision. *Tectonophysics*, 111, 25-39, doi: 10.1016/0040-1951(85)90064-2.

Caputo, M., Marten, R. & Mecham, B., 1988.The stress field due to mass anomalies in the Apennines, the Kermadec-Tonga Trench and the Rio Grande Rift. *Annales Tectonicae*, 2, 33-50.

Caputo, R., 2005. Stress variability and brittle tectonic structures. *Earth Sci. Rev*., 70, 103-127, doi: 10.1016/j.earscirev.2004.11.005.

Caputo, R. & Pavlides, S., 1993. Late Cainozoic geodynamic evolution of Thessaly and surroundings (central-northern Greece). *Tectonophys*., 223(3-4), 339-362.

Caputo, R. & Sato H., 1996. An integrated study to recent tectonics in Central Japan: seismological, geodetic, morphotectonic and structural data compared. *Tectonophys*., 262, 1-4, 133-157.

Carafa, M.M.C. & Barba, S., 2013. The stress field in Europe: optimal orientations with confidence limits. *Geophys. J. Int*., 193(2), 531-548.

Carafa, M.M., Tarabusi, G. & Kastelic, V., 2015. SHINE: Web application for determining the horizontal stress orientation. *Comp. Geosci*., 74, 39-49, doi: 10.1016/j.cageo.2014.10.001.

Cartwright, J.A. & Jackson, M.P.A., 2008. Initiation of gravitational collapse of an evaporite basin margin: the Messinian saline giant, Levant Basin, eastern Mediterranean. *Geol. Soc. Am. Bull.*, 120, 399-413, doi: 10.1130/B26081X.1.

Casas, A.M., Simon, J.L. & Seron, F.J., 1992. Stress deflection in a tectonic compressional field: a model for the northwestern Iberian Chain, Spain. *J. Geophys. Res.*, 97, 7183-7192.

Catalano, S., De Guidi, G., Monaco, C., Tortorici, G. & Tortorici, L., 2008. Active faulting and seismicity along the Siculo–Calabrian Rift Zone (southern Italy). *Tectonophys*., 453, 177-192, doi: 10.1016/j.tecto.2007.05.008

Catalano, S., Romagnoli, G. & Tortorici, G., 2010. Kinematics and dynamics of the Late Quaternary rift-flank deformation in the Hyblean Plateau (SE Sicily). *Tectonophys.*, 486, 1-14, doi: 10.1016/j.tecto.2010.01.013.

D'Agostino, N. & Selvaggi, G., 2004. Crustal motion along the Eurasia-Nubia plate boundary in the Calabrian Arc and Sicily and active extension in the Messina Straits from GPS measurements. *J. Geophys. Res. (1978–2012)*, 109(B11). doi: 10.1029/2004JB002998

De Guidi, G., Caputo, R. & Scudero, S., 2013. Regional and local stress field orientation inferred from quantitative analyses of extension joints: case study from southern Italy. *Tectonics*, 32(2), 239-251, doi: 10.1002/tect.20017.

De Guidi, G., Lanzafame, G., Palano, M., Puglisi, G., Scaltrito, A. & Scarfì, L., 2013. Multidisciplinary study of the Tindari Fault (Sicily, Italy) separating ongoing contractional and extensional compartments along the active Africa–Eurasia convergent boundary. *Tectonophys.*, 588, 1-17.

De Guidi, G., Barberi, G., Barreca, G., Bruno, V., Cultrera, F., Grassi, S., Imposa, S., Mattia, M., Monaco, C., Scarfì, L. & Scudero, S., 2015. Geological, seismological and geodetic evidence of active thrusting and folding south of Mt. Etna (eastern Sicily): Revaluation of "seismic efficiency" of the Sicilian Basal Thrust. *J. Geodyn*., 90, 32-41, doi: 10.1016/j.jog.2015.06.001.

Del Ben, A., Barnaba, C. & Taboga, A., 2008. Strike-slip systems as the main tectonic features in the Plio-Quaternary kinematics of the Calabrian Arc. *Marine Geophys. Res*., 29(1), 1-12. doi: 10.1007/s11001-007-9041-6.

Doglioni, C., Ligi, M., Scrocca, D., Bigi, S., Bortoluzzi, G., Carminati, E., & Riguzzi, F., 2012. The tectonic puzzle of the Messina area (Southern Italy): Insights from new seismic reflection data. *Scientific Reports*, 2, 970, doi: 10.1038/srep00970.

Fabbri, O. and Fournier, M., 1999. Extension in the southern Ryukyu are (Japan): link with oblique subduction and back are rifting. *Tectonics*, 18(3), 486-497.

Falà, F., 2011. Determinazione dei Meccanismi Focali e del Tensore dello Sforzo in Italia Meridionale. PhD thesis, Università di Catania.

Ferranti, L., Monaco, C., Morelli, D., Antonioli, F.& Maschio, L., 2008. Holocene activity of the Scilla Fault, Southern Calabria: Insights from coastal morphological and structural investigations. *Tectonophys*., 453(1-4), 74-93.

Gallais, F., Graindorge, D., Gutscher, M. A., & Klaeschen, D., 2013. Propagation of a lithospheric tear fault (STEP) through the western boundary of the Calabrian accretionary wedge offshore eastern Sicily (Southern Italy). *Tectonophys*., 602, 141-152, doi: 10.1016/j.tecto.2012.12.026.

Giampiccolo, E., Musumeci, C., Falà, F. & Gresta, S., 2008. Seismological investigations in the Gioia Tauro Basin (southern Calabria, Italy). *Ann. Geophys.*, 51(5/6), 769-799.

Ghisetti, F., 1979a. Evoluzione neotettonica dei principali sistemi di faglie della Calabria centrale. *Boll. Soc. Geol. It.*, 98,387-430.

Ghisetti, F., 1979b. Relazioni tra strutture e fasi trascorrenti e distensive lungo i sistemi Messina-Fiumefreddo, Tindari-Letojanni e Alia-Malvagna (Sicilia nord-orientale): uno studio microtettonico. *Geol. Rom*, 18, 23-58.

Harris, R.A., 1998. Introduction to special section: stress triggers, stress shadows, and implications for seismic hazard. *J. Geophys. Res*., 103, 24,347-24,358.

Heidbach, O., Rajabi, M., Cui, X., Fuchs, K., Müller, B., Reinecker, J. & Ziegler, M.O., 2018. The World Stress Map database release 2016: Crustal stress pattern across scales. *Tectonophys*., 744, 484-498.

Heidbach, O., Reinecker, J., Tingay, M., Müller, B., Sperner, B., Fuchs, K. & Wenzel, F., 2007. Plate boundary forces are not enough: second- and third-order stress patterns highlighted in the World Stress Map database. *Tectonics*, 26(6), TC6014. doi: 10.1029/2007TC002133.

Heidbach, O., Tingay, M., Barth, A., Reinecker, J., Kurfeß, D., & Müller, B., 2010. Global crustal stress pattern based on the World Stress Map database release 2008. *Tectonophysics*, 482, 3-15, doi: 10.1016/j.tecto.2009.07.023

Jaeger, J.C., Cook, N.G.W., and Zimmerman, R.W., 2007. Fundamentals of Rock Mechanics, 4th ed. Oxford: Blackwell.

Kanamori, H., & Anderson, D. L., 1975.Theoretical basis of some empirical relations in seismology. *Bull. Seism. Soc. Am*., 65(5), 1073-1095.

Larroque, J.M., Etchecopar, A. & Philip, H., 1987. Evidence for the permutation of stresses σ1 and σ2 in the Alpine foreland: the example of the Rhine graben. *Tectonophys.*, 144, 315-322.

Lavecchia, G., Ferrarini, F., De Nardis, R., Visini, F. & Barbano, M.S., 2007. Active thrusting as a possible seismogenic source in Sicily (Southern Italy): Some insights from integrated structural–kinematic and seismological data. *Tectonophys*., 445, 145-167. doi: 10.1016/j.tecto.2007.07.007

Maggini, M. & Caputo, R., 2020. Rheological behaviour in continental and oceanic subduction: inferences for the seismotectonics of the Aegean Region. *Turkish J. Earth Sci*., 29, 381-405, doi: 10.3906/yer-1909-4.

Maerten, L., Gillespie, P. & Pollard, D.D., 2002. Effects of local stress perturbation on secondary fault development. *J. Struct. Geol*., 24, 145-153.

McGarr, A., 1988. On the state of lithospheric stress in the absence of applied tectonic forces. *J. Geophys. Res.*, 93, B11, 13,609-13,617.

Mercier J.-L., 1976. La néotectonique. Ses méthodes et ses buts. Un exemple: l'Arc Egéen (Méditerranée orientale*). Rev. Géol. Dyn. Géogr. Phys*., XVIII (4), 323-346.

Mercier, J.L., Sebrier, M., Lavenu, A., Cabrera, J., Bellier, O., Dumont, J.-F. & Machare, J., 1992. Changes in the tectonic regime above a subduction zone of Andean type: the Andes of Peru and Bolivia during the Pliocene-Pleistocene. *J. Geophys. Res*., 97, B8, 11,945-11,982.

Meschis, M., Roberts, G. P., Mildon, Z.K., Robertson, J., Michetti, A.M., & Walker, J.F., 2019. Slip on a mapped normal fault for the 28th December 1908 Messina earthquake (Mw 7.1) in Italy. *Scientific Reports*, 9, 1-8, doi: 10.1038/s41598-019-42915-2.

Monaco, C., Tapponnier, P., Tortorici, L. & Gillot, P. Y., 1997. Late Quaternary slip rates on the Acireale-Piedimonte normal faults and tectonic origin of Mt. Etna (Sicily). *Earth Planet. Sci. Lett*., 147, 125-139.

Montone, P., Mariucci, M.T. & Pierdominici, S., 2012. The Italian present-day stress map. *Geophys. J. Int*., 189, 705-716.

Nakamura, K., 1977. Volcanoes as possible indicators of tectonic stress orientation—principle and proposal. *J. Volc. Geoth. Res.*, 2, 1-16, doi: 10.1016/0377-0273(77)90012-9.

Neri, G., Barberi, G., Oliva, G. & Orecchio, B., 2005. Spatial variations of seismogenic stress orientations in Sicily, south Italy. *Physics Earth Planet. Inter*., 148, 175-191. doi: 10.1016/j.pepi.2004.08.009.

Neri, G., Marotta, A.M., Orecchio, B., Presti, D., Totaro, C., Barzaghi, R. & Borghi, A., 2012. How lithospheric subduction changes along the Calabrian Arc in southern Italy: geophysical evidences. *Int. J. Earth Sci.*, 101, 1949-1969. doi: 10.1007/s00531-012-0762-7.

Neri, G., Orecchio, B., Scolaro, S. & Totaro, C., 2020. Major Earthquakes of Southern Calabria, Italy, Into the Regional Geodynamic Context. *Frontiers in Earth Science*, 8:579846, doi: 10.3389/feart.2020.579846

Nüchter, J.A. & Stöckhert, B., 2008. Coupled stress and pore fluid pressure changes in the middle crust: vein record of coseismic loading and postseismic stress relaxation. *Tectonics*, 27, TC1007, doi: 10.1029/2007TC002180.

Palano, M., 2015. On the present-day crustal stress, strain-rate fields and mantle anisotropy pattern of Italy. *Geophys. J. Int.*, 200, 967-983. doi: 10.1093/gji/ggu451.

Palano, M., Ferranti, L., Monaco, C., Mattia, M., Aloisi, M., Bruno, V., Cannavò, F. & Siligato, G., 2012. GPS velocity and strain fields in Sicily and southern Calabria, Italy: updated geodetic constraints on tectonic block interaction in the central Mediterranean. *J. Geophys. Res*., 117(B7). doi: 10.1029/2012JB009254.

Palano, M., Schiavone, D., Loddo, M., Neri M., Presti, D., Quarto, R., Totaro, C. & Neri, G., 2015. Active upper crust deformation pattern along the southern edge of the Tyrrhenian subduction zone (NE Sicily): Insights from a multidisciplinary approach. *Tectonophys*., 657, 205-218. doi:10.1016/j.tecto.2015.07.005.

Peterson, M.S. & Wong, T.F., 2005. Experimental Rock Deformation – The Brittle Field, 2nd ed. Springer-Verlag, Berlin

Pierdominici, S. & Heidbach, O., 2012. Stress field of Italy-Mean stress orientation at different depths and wave-length of the stress pattern. *Tectonophys*., 532, 301-311, doi: 10.1016/j.tecto.2012.02.018.

Polonia, A., Torelli, L., Gasperini, L. & Mussoni, P., 2012.Active faults and historical earthquakes in the Messina Straits area (Ionian Sea). *Nat. Haz. Earth Sys.Sci.*, 12, 2311-2328. doi: 10.5194/nhess-12-2311-2012.

Polonia, A., Torelli, L., Mussoni, P., Gasperini, L., Artoni, A. & Klaeschen, D., 2011. The Calabrian Arc subduction complex in the Ionian Sea: Regional architecture, active deformation, and seismic hazard. *Tectonics*, 30, TC5018. doi: 10.1029/2010TC002821.

Presti, D., Billi, A., Orecchio, B., Totaro, C., Faccenna, C. & Neri, G., 2013. Earthquake focal mechanisms, seismogenic stress, and seismotectonics of the Calabrian Arc, Italy. *Tectonophys*., 602, 153-175. doi: 10.1016/j.tecto.2013.01.030.

Roberts, G.P. & Michetti, A.M., 2004. Spatial and temporal variations in growth rates along active normal fault Systems: an example from Lazio-Abruzzo, central Italy. *J. Struct. Geol*., 26, 339-376.

Scarfì, L., Messina, A. & Cassisi, C., 2013. Sicily and Southern Calabria focal mechanism database: a valuable tool for local and regional stress field determination. *Ann. Geophys*., 56, D0109.

Scarfì, L., Barberi, G., Musumeci, C. & Patanè, D., 2016. Seismotectonics of northeastern Sicily and southern Calabria (Italy): New constraints on the tectonic structures featuring in a crucial sector for the central Mediterranean geodynamics. *Tectonics*, 35, 812-830.

Scarfi, L., Barberi, G., Barreca, G., Cannavo, F., Koulakov, I. & Patane, D., 2018. Slab narrowing in the Central Mediterranean: the Calabro-Ionian subduction zone as imaged by high resolution seismic tomography. *Sci. Rep. 2018* (8), 5178, doi: 10.1038/s41598-018-23543-8.

Sperner, B., Müller, B., Heidbach, O., Delvaux, D., Reinecker, J. &Fuchs, K., 2003. Tectonic stress in the Earth's crust: Advances in the World Stress Map project. *Geol. Soc., London, Special Publications*, 212, 101-116.

Soumaya, A., BenAyed, N., Delvaux, D. & Mohamed, G., 2015. Spatial variation of Present-day stress field and tectonic regime in Tunisia and surroundings from formal inversion of focal mechanisms: geodynamic implications for Central Mediterranean. *Tectonics*, 34, 1154-1180. doi: 10.1002/2015TC003895.

Steacy, S., Gomberg, J. & Cocco, M., 2005. Introduction to special section: Stress transfer, earthquake triggering, and time-dependent seismic hazard. *J. Geophys. Res*., 110, B05S01. doi: 10.1029/2005JB003692.

Tortorici, L., Monaco, C., Tansi, C. & Cocina, O., 1995. Recent and active tectonics in the Calabrian arc (Southern Italy). *Tectonophys*., 243, 37-55.

Vigneresse, J.-L., Tikoff, B. & Améglio, L., 1999. Modification of the regional stress field by magma intrusion and formation of tabular granitic plutons. *Tectonophys*., 302, 203-234.

Zoback, M.L., 1992. First- and second-order patterns of stress in the lithosphere: the world stress map project. *J. Geophys. Res*., 97, B8, 11,703-11,728.

Zoback, M.L. & Zoback, M., 1989. Tectonic stress field of the conterminous United States. In: L.C. Pakiser, W.D. Mooney (Eds.), *Geophysical Framework of the Continental United States*. *Geol. Soc. Am. Mem*, Boulder, Colorado, 523-539.

Appendix A

Table A1. List of the stress indicators. Type: FM = Focal Mechanism, also the corresponding earthquake magnitude (M) and depth (Depth) are provided; F = indicators from main fault planes; J = set of extensional joints. Sources: Bill06 = Billi *et al.*, 2006; DeGui13 = De Guidi *et al.*, 2013; Fal11 = Falà, 2011; Ferr08 = Ferranti *et al.*, 2008; Ghi79a =Ghisetti, 1979; Giam08 = Giampiccolo *et al.*, 2008; Ner05 = Neri *et al.*, 2005; Pre13 = Presti *et al.*, 2013; Scar13 = Scarfì *et al.*, 2013; Tor95 = Tortorici *et al.*, 1995. Data from Table 4 are listed as "this work".

ID	Type	M	Lat_N	Long_E	Depth	P strike	P plunge	T strike	T plunge	B strike	B plunge	I_Q	I_V	W	Source
1	FM	2.8	37,80	15,46	10.05	182	38	308	38	65	30	L	M	0.125	Fal11
2	FM	3.5	37,80	15,04	0.38	33	4	126	32	297	58	M	M	0.25	Scar13
3	FM	3.5	37,80	15,06	12,00	49	42	302	18	195	43	H	M	0.5	Pre13
4	FM	3.1	37,80	15,12	6.7	51	38	307	17	198	47	H	M	0.5	Pre13
5	FM	2.8	37,80	15,07	2,00	53	11	321	8	196	76	H	M	0.5	Pre13
6	FM	2.9	37,80	15,55	3.5	111	48	299	42	205	4	M	M	0.25	Ner05
7	FM	2.7	37,80	14,83	7.96	255	70	63	20	154	4	M	M	0.25	Scar13
8	FM	3.6	37,80	15,04	0.12	37	13	303	15	166	70	H	M	0.5	Scar13
9	FM	3.4	37,80	14,94	22.87	303	18	34	3	133	72	H	M	0.5	Scar13
10	FM	2.7	37,80	14,91	26.94	333	32	218	34	94	40	H	M	0.5	Scar13
11	FM	2.7	37,80	14,91	27.08	340	19	232	42	88	42	L	M	0.125	Scar13
12	J	-	37,80	15,24	-	266	87	154	1	64	3	H	M	0.5	this work
13	FM	3.1	37,80	14,91	25.03	319	29	205	37	76	40	H	M	0.5	Scar13
14	FM	3.2	37,80	14,93	24.22	322	15	228	15	95	69	H	M	0.5	Scar13
15	FM	2.8	37,80	15,61	6.75	22	18	291	3	192	72	H	M	0.5	Scar13
16	FM	2.4	37,80	15,04	25.01	133	14	227	14	360	70	H	M	0.5	Ner05
17	FM	3.4	37,80	14,91	25.5	322	13	228	15	91	70	H	M	0.5	Scar13
18	FM	3.5	37,80	14,93	21.34	292	15	198	15	65	69	H	M	0.5	Scar13
19	FM	4	37,80	14,94	20.35	309	20	211	21	79	60	H	H	1	Scar13
20	FM	3.1	37,81	14,92	23.2	301	6	210	8	67	80	H	M	0.5	Scar13
21	FM	3.5	37,81	14,89	23.68	318	41	92	39	204	25	M	M	0.25	Scar13
22	FM	2.7	37,81	15,04	15.3	319	36	184	45	68	25	M	M	0.25	Ner05
23	FM	3	37,81	15,09	2.59	35	35	179	49	292	18	H	M	0.5	Scar13
24	FM	3.5	37,81	15,11	0.64	60	1	150	1	285	89	H	M	0.5	Scar13
25	FM	3.3	37,81	14,89	24.74	330	18	208	58	69	25	H	M	0.5	Scar13
26	FM	3.6	37,81	15,11	-0.38	63	14	157	14	290	70	H	M	0.5	Scar13
27	FM	2.9	37,81	15,04	15.4	102	5	224	81	11	8	M	M	0.25	Ner05
28	FM	3.3	37,81	15,11	-0.33	53	56	153	7	248	33	H	M	0.5	Scar13
29	FM	2.8	37,81	14,92	28.22	316	28	47	1	139	62	H	M	0.5	Scar13

30	FM	3.3	37,81	15,07	-0.66	18	64	150	18	246	18	H	M	0.5	Scar13
31	FM	3.3	37,81	15,10	-0.62	45	45	156	20	263	38	H	M	0.5	Scar13
32	FM	2.5	37,81	15,04	15.3	15	52	247	26	143	26	M	M	0.25	Ner05
33	FM	3.6	37,81	14,84	23.33	52	51	194	32	296	19	H	M	0.5	Ner05
34	FM	2.8	37,81	15,10	0.93	64	14	318	49	165	38	H	M	0.5	Scar13
35	FM	3.6	37,81	14,88	22.82	250	5	69	85	340	0	M	M	0.25	Ner05
36	FM	3.1	37,81	14,95	19.31	341	33	214	42	93	30	H	M	0.5	Scar13
37	FM	3	37,82	14,84	24.1	284	76	39	6	130	13	H	M	0.5	Scar13
38	FM	3.2	37,83	14,88	25.35	339	55	119	28	220	19	H	M	0.5	Scar13
39	FM	2.7	37,83	15,03	17.7	322	38	88	38	205	30	M	M	0.25	Ner05
40	FM	2.5	37,84	15,43	7.81	182	41	295	24	46	39	M	M	0.25	Fal11
41	FM	2.8	37,84	14,90	25.73	344	60	77	2	168	30	L	M	0.125	Scar13
42	FM	3.2	37,84	14,89	26.23	331	45	113	38	220	20	H	M	0.5	Scar13
43	FM	3.4	37,84	14,89	26.09	346	47	112	29	220	29	H	M	0.5	Scar13
44	FM	3.8	37,84	15,38	16.8	157	15	273	59	60	27	H	M	0.5	Scar13
45	FM	3.1	37,84	14,85	24.31	351	31	100	29	224	45	H	M	0.5	Scar13
46	FM	3	37,84	15,56	6.9	355	7	85	7	220	80	H	M	0.5	Pre13
47	FM	3.3	37,84	14,94	23.71	172	5	294	81	81	8	H	M	0.5	Ner05
48	FM	4	37,84	14,88	26.68	333	49	79	14	180	38	H	H	1	Scar13
49	FM	3.3	37,85	14,89	25.38	328	49	74	14	175	38	M	M	0.25	Scar13
50	FM	2.8	37,85	14,97	12.5	154	76	36	7	305	13	M	M	0.25	Ner05
51	FM	2.7	37,85	14,93	25.59	301	25	33	4	132	65	H	M	0.5	Scar13
52	FM	3.4	37,85	14,99	25.76	312	21	45	7	152	68	H	M	0.5	Scar13
53	FM	2.8	37,85	14,98	25.08	319	8	51	8	185	79	H	M	0.5	Scar13
54	FM	2.7	37,86	15,12	17.58	353	32	238	34	141	40	H	M	0.5	Scar13
55	FM	3.3	37,86	15,38	8.9	28	8	292	35	129	54	H	M	0.5	Scar13
56	FM	2.3	37,86	14,94	26.44	101	21	199	21	330	60	H	M	0.5	Ner05
57	FM	3	37,86	15,51	21.5	116	42	304	48	210	4	H	M	0.5	Ner05
58	FM	3	37,87	14,94	26.92	314	22	68	44	206	38	H	M	0.5	Scar13
59	FM	2.7	37,87	14,98	24.5	311	31	46	9	151	57	M	M	0.25	Ner05
60	FM	3.1	37,87	15,01	6.21	208	71	60	17	327	10	H	M	0.5	Ner05
61	FM	2.6	37,87	15,68	32.22	23	10	173	78	292	6	L	M	0.125	Fal11
62	FM	3	37,87	15,36	9.93	28	21	295	7	188	68	H	M	0.5	Scar13
63	FM	2.6	37,88	15,57	25.98	183	49	76	14	334	38	M	M	0.25	Ner05
64	FM	3.5	37,88	14,87	29.34	341	21	73	7	181	69	H	M	0.5	Scar13
65	F	-	37,88	15,30	-	167	75	313	13	45	8	H	H	1	Ghi79b
66	FM	3.4	37,88	14,90	26.9	73	29	200	47	326	29	M	M	0.25	Ner05
67	FM	2.9	37,89	14,99	7.26	324	49	164	40	66	10	H	M	0.5	Ner05
68	FM	2.9	37,89	14,98	27.79	321	31	62	17	177	54	M	M	0.25	Scar13
69	FM	3	37,90	14,81	12.71	291	82	57	5	148	6	H	M	0.5	Scar13
70	FM	3.3	37,90	15,45	6.21	118	79	267	10	358	6	H	M	0.5	Scar13
71	FM	3.2	37,90	15,61	7.86	140	69	266	13	360	16	M	M	0.25	Scar13
72	FM	2.7	37,90	15,45	9.38	132	61	275	24	12	16	M	M	0.25	Scar13
73	FM	2.9	37,91	15,62	7.98	152	63	273	15	9	22	L	M	0.125	Scar13

74	FM	4.4	37,92	15,18	10,00	20	13	280	37	126	50	H	H	1	Pre13
75	FM	2.7	37,92	14,90	28.71	164	74	31	11	299	11	H	M	0.5	Scar13
76	FM	2.7	37,93	14,89	25.91	328	54	168	34	72	10	M	M	0.25	Scar13
77	FM	2.7	37,95	14,90	26.36	339	49	151	41	244	4	M	M	0.25	Scar13
78	FM	3.2	37,96	15,50	8.41	246	18	152	10	33	69	H	M	0.5	Ner05
79	FM	2.8	37,96	15,53	9.95	68	47	300	29	193	28	M	M	0.25	Fal11
80	FM	3.1	37,97	14,93	20.9	124	28	221	13	33	59	M	M	0.25	Ner05
81	FM	2.9	37,97	15,14	9.68	245	51	338	2	70	39	M	M	0.25	Fal11
82	FM	3.7	37,98	15,40	11.4	124	58	218	2	309	32	M	M	0.25	Ner05
83	FM	2.8	37,99	15,10	8.5	238	81	117	5	26	8	H	M	0.5	Scar13
84	FM	3	37,99	15,13	5.55	266	55	11	10	106	33	M	M	0.25	Fal11
85	FM	3.3	37,99	15,10	9.5	196	69	296	4	28	21	H	M	0.5	Scar13
86	FM	3.3	37,99	15,06	10.3	239	49	338	8	75	40	H	M	0.5	Pre13
87	FM	2.3	38,00	15,17	10.17	200	80	20	10	290	0	H	M	0.5	DeGui13
88	FM	3.8	38,01	15,92	9.75	127	69	14	8	281	19	H	M	0.5	Scar13
89	FM	3.7	38,01	14,80	7.5	104	64	360	7	267	25	H	M	0.5	Pre13
90	FM	3.3	38,01	14,81	9.57	131	68	224	1	314	22	H	M	0.5	Scar13
91	FM	3.3	38,02	14,80	9.35	273	55	152	20	51	28	H	M	0.5	Scar13
92	FM	2.7	38,02	15,06	16.6	139	67	277	18	12	15	H	M	0.5	DeGui13
93	FM	2.9	38,03	15,08	9.65	26	76	271	6	180	13	H	M	0.5	Scar13
94	FM	2.3	38,03	15,05	11.9	66	72	181	8	273	16	H	M	0.5	DeGui13
95	FM	2.7	38,03	15,12	8.15	141	60	327	30	236	3	H	M	0.5	Scar13
96	FM	2.7	38,03	14,81	8.61	245	69	11	13	105	16	H	M	0.5	Scar13
97	FM	2.7	38,03	15,10	12.75	330	79	150	11	60	0	H	M	0.5	Scar13
98	FM	3.1	38,04	15,04	14.14	44	83	138	0	228	7	H	M	0.5	Scar13
99	FM	3.7	38,04	15,11	13.15	130	70	322	20	231	4	H	M	0.5	Scar13
100	FM	2.7	38,04	15,09	9.33	228	76	324	1	54	14	H	M	0.5	Scar13
101	FM	2.7	38,04	15,71	16.53	110	37	224	29	341	40	H	M	0.5	Scar13
102	FM	2.2	38,05	15,05	7.81	228	76	344	6	75	13	H	M	0.5	DeGui13
103	FM	2.3	38,06	14,98	12.66	34	81	153	5	244	8	H	M	0.5	DeGui13
104	FM	2.9	38,06	15,09	12.44	111	72	325	15	232	10	H	M	0.5	Scar13
105	FM	2.7	38,07	15,13	7.2	202	79	53	10	322	9	H	M	0.5	Scar13
106	FM	2.1	38,07	15,11	11.63	5	72	121	8	213	16	H	M	0.5	DeGui13
107	FM	3.6	38,07	15,08	30,00	25	22	117	4	217	68	H	M	0.5	Pre13
108	J	-	38,07	15,48	-	207	79	112	1	21	11	H	M	0.5	this work
109	FM	2.4	38,08	15,04	20.72	145	52	52	2	321	39	H	M	0.5	DeGui13
110	J	-	38,08	15,71	-	313	76	167	12	75	8	M	M	0.25	this work
111	FM	3.3	38,08	15,15	22.39	90	90	195	0	285	0	H	M	0.5	Ner05
112	FM	2.7	38,08	14,91	15.62	169	60	343	30	75	3	H	M	0.5	Scar13
113	FM	3.5	38,09	15,29	8.85	39	46	133	5	228	44	H	M	0.5	Scar13
114	FM	2.8	38,09	15,57	6.09	196	83	102	0	12	7	H	M	0.5	Scar13
115	FM	2.5	38,09	15,13	14.08	63	74	166	4	257	15	H	M	0.5	DeGui13
116	FM	3.3	38,09	15,57	6.13	225	89	103	1	13	4	H	M	0.5	Scar13
117	FM	2.1	38,09	15,17	34.9	267	49	14	14	116	38	H	M	0.5	DeGui13

118	FM	2.6	38,09	15,09	8.89	330	80	150	10	60	0	H	M	0.5	DeGui13
119	FM	2.7	38,10	14,93	14.15	108	39	353	27	239	39	H	M	0.5	Scar13
120	F	-	38,10	15,21	-	101	65	282	25	192	0	L	M	0.125	this work
121	FM	4.4	38,10	14,92	18.52	193	1	283	38	102	52	H	H	1	Scar13
122	J	-	38,10	15,21	-	7	56	102	4	195	34	H	M	0.5	this work
123	F	-	38,10	15,21	-	113	74	291	16	21	1	L	M	0.125	this work
124	FM	5.6	38,10	16,03	33,00	281	77	167	5	76	12	H	H	1	Pre13
125	F	-	38,10	15,21	-	156	63	341	27	250	2	M	M	0.25	this work
126	F	-	38,10	15,21	-	164	77	309	11	41	7	L	M	0.125	this work
127	FM	3.1	38,10	15,16	12.96	116	72	330	15	237	10	H	M	0.5	Scar13
128	F	-	38,10	15,08	-	282	11	13	3	120	79	L	M	0.125	this work
129	F	-	38,10	15,21	-	306	67	127	23	37	0	L	M	0.125	this work
130	F	-	38,10	15,21	-	108	78	278	12	9	2	L	M	0.125	this work
131	FM	2.8	38,10	15,15	14.75	122	74	322	15	231	5	H	M	0.5	Scar13
132	FM	2.7	38,10	15,21	10.43	123	61	327	27	232	10	M	M	0.25	Fal11
133	FM	2.7	38,11	14,91	17.02	168	11	269	42	67	46	H	M	0.5	Scar13
134	FM	2.7	38,11	15,20	12.27	10	80	190	10	280	0	H	M	0.5	Fal11
135	FM	2.8	38,11	15,21	10.4	184	76	299	6	30	13	M	M	0.25	Scar13
136	FM	3	38,11	15,15	10.1	310	79	130	11	40	0	M	M	0.25	Scar13
137	FM	4.5	38,11	14,91	19.38	176	29	290	37	59	40	H	H	1	Scar13
138	FM	2.9	38,11	14,92	17.14	353	25	224	53	96	25	H	M	0.5	Scar13
139	J	-	38,11	15,72	-	352	84	157	6	247	2	M	M	0.25	this work
140	J	-	38,11	15,12	-	169	46	264	4	358	44	M	M	0.25	this work
141	FM	2.9	38,11	15,65	10.63	16	56	272	9	176	32	M	M	0.25	Scar13
142	FM	2.6	38,11	15,22	8.15	153	74	313	15	44	5	H	M	0.5	DeGui13
143	FM	2.5	38,11	14,92	29.49	181	51	301	22	45	30	M	M	0.25	Fal11
144	FM	2.3	38,11	15,21	11.61	260	76	354	2	84	14	H	M	0.5	DeGui13
145	F	-	38,11	15,21	-	317	57	134	33	225	2	L	M	0.125	this work
146	F	-	38,12	15,05	-	289	79	95	10	185	3	H	H	1	DeG13
147	FM	2.4	38,12	15,20	9.95	153	74	313	15	44	5	H	M	0.5	DeGui13
148	FM	2.2	38,12	15,18	10.29	310	85	130	5	40	0	H	M	0.5	DeGui13
149	J	-	38,12	15,21	-	26	23	294	5	192	67	M	M	0.25	this work
150	F	-	38,12	15,21	-	285	73	108	17	18	1	M	M	0.25	this work
151	FM	2.5	38,12	14,92	26.48	109	63	357	11	262	25	H	M	0.5	DeGui13
152	FM	2.6	38,12	15,12	12,00	9	61	112	8	206	28	M	M	0.25	Ner05
153	FM	2.3	38,12	15,23	11.7	125	75	305	15	35	0	H	M	0.5	DeGui13
154	FM	7	38,12	15,60	10,00	173	69	281	7	13	20	M	H	0.5	Ner05
155	J	-	38,12	15,74	-	100	86	338	2	248	3	H	M	0.5	this work
156	FM	3.3	38,12	15,19	12.63	63	72	325	6	232	17	H	M	0.5	Scar13
157	FM	3.1	38,12	15,23	9,00	331	79	131	10	222	4	H	M	0.5	DeGui13
158	J	-	38,12	15,72	-	42	76	161	7	253	12	M	M	0.25	this work
159	FM	2.2	38,12	14,95	18.86	140	74	6	11	273	11	H	M	0.5	DeGui13
160	FM	2.5	38,12	15,14	11.88	197	69	296	4	27	21	H	M	0.5	DeGui13
161	J	-	38,12	14,96	-	30	79	299	0	209	11	H	M	0.5	this work

162	FM	2.1	38,12	14,96	19.54	104	74	331	11	238	11	H	M	0.5	DeGui13
163	FM	2.2	38,13	15,12	17.43	68	82	303	5	212	7	H	M	0.5	DeGui13
164	FM	3.7	38,13	15,19	9.17	80	79	312	7	221	9	H	M	0.5	Scar13
165	J	-	38,13	15,18	-	233	75	347	6	78	13	M	M	0.25	this work
166	F	-	38,13	15,18	-	104	83	265	7	355	2	M	M	0.25	this work
167	FM	2.6	38,13	15,14	8.66	82	76	326	6	235	13	H	M	0.5	DeGui13
168	FM	3.4	38,13	15,83	9.05	175	69	301	13	35	16	H	M	0.5	Scar13
169	FM	2.6	38,13	15,10	10,00	34	55	132	5	225	35	H	M	0.5	Pre13
170	FM	2.6	38,13	15,30	9.96	40	56	179	27	279	19	M	M	0.25	Fal11
171	FM	3	38,13	15,13	14.07	102	81	223	5	314	8	H	M	0.5	Ner05
172	FM	2.3	38,13	14,96	21.93	152	70	317	20	49	4	H	M	0.5	DeGui13
173	FM	2.7	38,13	15,18	10.5	335	18	88	51	232	38	M	M	0.25	Ner05
174	FM	2.9	38,14	15,14	13.91	150	80	330	10	64	0	H	M	0.5	Scar13
175	FM	4.4	38,14	15,20	10.1	25	74	135	6	227	16	H	H	1	Scar13
176	FM	2.5	38,14	15,12	14.31	326	85	145	6	55	0	H	M	0.5	DeGui13
177	FM	3	38,14	15,15	13.44	250	72	134	8	42	16	H	M	0.5	Ner05
178	FM	3	38,14	15,14	9.44	285	85	105	5	15	0	H	M	0.5	Scar13
179	FM	2.7	38,14	15,07	4.61	299	80	120	10	30	0	H	M	0.5	DeGui13
180	FM	3.1	38,14	15,30	8.2	326	77	187	9	96	8	M	M	0.25	Fal11
181	FM	3.1	38,14	15,18	9.1	58	67	324	2	233	23	H	M	0.5	Pre13
182	FM	3.1	38,14	15,18	10.5	82	61	331	11	236	26	H	M	0.5	Pre13
183	FM	2.7	38,14	15,13	12.64	162	80	305	8	36	6	M	M	0.25	Scar13
184	F	-	38,14	15,66	-	154	71	298	16	31	11	H	H	1	Tor95
185	FM	2.9	38,14	15,03	15.16	85	69	319	13	225	16	H	M	0.5	Scar13
186	FM	3.4	38,14	15,17	13.63	145	90	145	0	235	0	H	M	0.5	Scar13
187	FM	2.7	38,14	15,13	7.67	135	90	135	0	225	0	H	M	0.5	Scar13
188	J	-	38,14	15,05	-	185	89	49	1	319	1	H	M	0.5	this work
189	J	-	38,14	15,05	-	0	0	319	1	0	0	H	L	0.25	this work
190	FM	3.1	38,14	15,19	14.17	24	69	284	4	193	21	M	M	0.25	Fal11
191	FM	2.9	38,14	15,11	13.81	99	82	333	5	242	6	H	M	0.5	Scar13
192	FM	2.9	38,15	15,03	14.55	59	57	306	14	208	29	H	M	0.5	Scar13
193	FM	2.8	38,15	15,19	11.69	36	56	292	9	196	32	H	M	0.5	Scar13
194	FM	2.3	38,15	15,17	11.53	300	80	120	10	30	0	H	M	0.5	DeGui13
195	J	-	38,15	14,96	-	72	68	336	2	245	22	H	M	0.5	this work
196	FM	2.8	38,15	14,95	17.39	1	23	106	31	241	50	H	M	0.5	Scar13
197	FM	3	38,15	15,03	14.7	74	62	301	20	204	19	H	M	0.5	Scar13
198	FM	2.7	38,15	14,95	17.3	351	6	106	76	260	13	H	M	0.5	Scar13
199	FM	3.3	38,15	15,62	9.47	38	44	284	22	176	38	H	M	0.5	Scar13
200	FM	3.3	38,15	14,95	8.35	120	51	27	2	296	39	H	M	0.5	DeGui13
201	FM	3.1	38,16	15,11	14.92	194	33	299	21	55	49	H	M	0.5	Ner05
202	FM	2.8	38,16	15,07	8.98	256	60	120	22	22	19	L	M	0.125	Fal11
203	FM	2.7	38,16	15,15	9.65	13	77	153	10	245	8	H	M	0.5	Scar13
204	FM	3.1	38,16	15,79	13.26	145	70	337	20	246	4	H	M	0.5	Scar13
205	J	-	38,16	14,96	-	108	77	258	11	349	6	H	M	0.5	this work

206	FM	4.2	38,16	14,91	24.12	139	67	277	18	12	15	H	H	1	Ner05
207	FM	2.7	38,17	14,90	27.85	122	66	224	5	317	24	H	M	0.5	DeGui13
208	FM	4.5	38,17	15,06	33,00	178	77	301	7	32	11	H	H	1	Pre13
209	FM	2.8	38,17	15,20	9.42	16	68	109	1	199	22	H	M	0.5	Scar13
210	FM	3.5	38,17	15,94	14.11	44	72	161	9	254	16	H	M	0.5	Scar13
211	FM	4	38,18	15,57	9.65	143	74	303	15	34	5	H	H	1	Scar13
212	FM	2.8	38,18	15,03	12,00	213	31	25	59	121	4	M	M	0.25	Ner05
213	FM	3.2	38,18	15,09	6.73	16	14	286	0	196	76	H	M	0.5	Scar13
214	FM	2.8	38,18	15,16	12.97	196	69	296	4	28	21	H	M	0.5	Scar13
215	FM	3	38,18	15,22	17,00	353	55	113	20	214	28	M	M	0.25	Ner05
216	FM	2.6	38,18	14,90	24.6	354	8	107	70	261	19	M	M	0.25	Ner05
217	F	-	38,19	15,32	-	70	63	245	27	340	0	L	M	0.125	this work
218	FM	2	38,19	15,17	11.57	5	68	131	13	225	17	H	L	0.25	DeGui13
219	FM	3.1	38,19	15,16	13.26	63	44	309	22	201	38	H	M	0.5	Scar13
220	FM	2.3	38,19	15,17	10.71	272	77	132	11	41	8	H	M	0.5	DeGui13
221	FM	3.4	38,19	15,12	10,00	338	3	247	27	80	76	H	M	0.5	Pre13
222	F	-	38,19	16,14	-	60	72	236	18	326	1	H	M	0.5	this work
223	FM	2.8	38,19	15,19	9.87	15	51	282	2	190	39	H	M	0.5	Scar13
224	FM	2.6	38,19	15,16	9.12	80	81	203	5	294	8	H	M	0.5	Ner05
225	FM	2.7	38,19	15,17	14.93	216	66	329	9	63	22	M	M	0.25	Fal11
226	FM	2.5	38,20	15,17	14.43	59	71	304	7	212	17	M	M	0.25	Fal11
227	FM	3.2	38,20	15,17	14.35	345	86	130	3	222	2	M	M	0.25	Scar13
228	FM	2.5	38,20	15,18	13.1	29	62	142	11	237	25	M	M	0.25	Fal11
229	FM	2.6	38,20	15,87	2,00	113	42	332	41	223	21	H	M	0.5	Pre13
230	FM	2.8	38,21	15,22	14.32	186	63	298	11	33	24	H	M	0.5	Scar13
231	J	-	38,21	15,67	-	252	85	60	5	150	1	H	M	0.5	this work
232	FM	2.5	38,21	15,06	16.34	31	40	271	30	157	34	H	M	0.5	DeGui13
233	FM	3.8	38,21	15,12	14.85	189	19	287	25	66	58	H	M	0.5	Scar13
234	FM	3	38,21	15,18	14.36	202	35	298	8	39	54	H	M	0.5	Scar13
235	J	-	38,21	15,69	-	243	87	70	3	340	0	M	M	0.25	this work
236	FM	2.8	38,21	15,18	13.6	76	10	344	11	207	75	H	M	0.5	Scar13
237	J	-	38,21	15,69	-	342	78	90	4	181	11	M	M	0.25	this work
238	FM	3.5	38,22	14,85	17.85	340	11	249	3	144	79	H	M	0.5	Scar13
239	FM	2.6	38,22	15,07	10.4	347	58	103	15	201	27	M	M	0.25	Ner05
240	FM	4.2	38,22	15,19	13.81	184	76	299	6	30	13	H	H	1	Scar13
241	FM	3.7	38,23	14,85	13.68	5	62	263	7	169	27	H	M	0.5	Scar13
242	FM	2.9	38,23	15,09	12.03	35	49	127	2	219	41	H	M	0.5	Scar13
243	FM	2.7	38,23	15,13	10,00	5	65	185	25	275	0	H	M	0.5	DeGui13
244	FM	3	38,24	15,11	14.59	203	11	304	42	104	40	H	M	0.5	Scar13
245	FM	2.9	38,24	15,67	13.91	338	55	239	6	148	35	H	M	0.5	Scar13
246	FM	3	38,25	15,51	21.5	76	8	321	72	168	16	H	M	0.5	Ner05
247	FM	3.2	38,25	15,67	13.31	343	54	241	9	145	35	H	M	0.5	Scar13
248	FM	3	38,25	15,08	12.1	200	17	298	25	79	59	H	M	0.5	Scar13
249	F	-	38,25	15,70	-	213	65	327	11	61	23	H	H	1	Ferr08

250	J	-	38,25	16,26	-	88	83	336	3	246	6	H	M	0.5	this work
251	FM	2.8	38,26	15,14	10.96	11	68	104	1	194	22	H	M	0.5	Scar13
252	FM	2.8	38,26	15,14	9.09	359	10	94	25	249	63	H	M	0.5	Scar13
253	FM	1.7	38,26	16,02	18.61	247	55	127	19	26	28	M	L	0.125	Giam08
254	FM	2.8	38,26	15,14	10.81	315	68	81	13	175	17	H	M	0.5	Scar13
255	FM	1.5	38,26	16,04	12.8	251	51	128	24	24	29	H	L	0.25	Giam08
256	FM	3.3	38,26	15,13	11.13	343	76	79	1	169	14	H	M	0.5	Scar13
257	FM	1.9	38,26	16,02	18.87	360	69	126	13	220	16	M	L	0.125	Giam08
258	FM	1.5	38,26	16,02	19.21	221	51	98	24	354	29	H	L	0.25	Giam08
259	FM	2.4	38,26	16,02	18.66	240	53	142	6	48	36	H	M	0.5	Giam08
260	FM	2.1	38,26	16,02	18.66	355	69	121	13	215	16	M	M	0.25	Giam08
261	F	-	38,26	15,87	-	218	64	315	4	47	26	H	H	1	Tor95
262	FM	1.4	38,26	16,03	18.27	223	14	317	14	90	70	H	L	0.25	Giam08
263	FM	2.2	38,26	16,03	18.66	225	45	114	20	7	38	H	M	0.5	Giam08
264	FM	1.2	38,26	16,04	14.29	233	61	77	27	342	10	M	L	0.125	Giam08
265	FM	1.4	38,26	16,02	19.11	237	51	97	32	354	20	L	L	0.0625	Giam08
266	FM	1.6	38,26	16,04	14.16	238	61	82	27	347	10	M	L	0.125	Giam08
267	FM	1.9	38,26	16,02	19.28	240	53	142	6	48	36	M	L	0.125	Giam08
268	FM	1	38,26	16,04	14.91	233	61	77	27	342	10	M	L	0.125	Giam08
269	FM	2.2	38,26	16,03	18.64	246	51	123	24	19	29	H	M	0.5	Giam08
270	FM	1.5	38,26	16,04	14.53	265	56	126	27	26	19	M	L	0.125	Giam08
271	FM	2.1	38,26	16,04	15.39	322	47	90	29	197	28	H	M	0.5	Giam08
272	FM	1.6	38,26	16,02	19.02	360	69	126	13	220	16	L	L	0.0625	Giam08
273	FM	2	38,26	16,02	19.33	41	18	307	10	190	69	H	L	0.25	Giam08
274	FM	1.5	38,26	16,02	18.94	215	45	104	20	357	38	M	L	0.125	Giam08
275	FM	1	38,26	16,03	19.1	221	51	98	24	354	29	M	L	0.125	Giam08
276	FM	1.3	38,26	16,03	18.1	229	47	104	29	356	29	H	L	0.25	Giam08
277	FM	1.5	38,26	16,03	18.08	231	51	108	24	4	29	L	L	0.0625	Giam08
278	FM	1.6	38,26	16,03	19.54	237	51	97	32	354	20	L	L	0.0625	Giam08
279	FM	0.8	38,26	16,04	13.29	325	45	76	20	183	38	M	L	0.125	Giam08
280	J	-	38,26	15,95	-	216	85	112	1	22	5	H	M	0.5	this work
281	F	-	38,26	15,95	-	116	82	296	8	206	0	M	M	0.25	this work
282	FM	2.8	38,26	15,13	12,00	7	44	272	6	176	46	H	M	0.5	Scar13
283	FM	2.2	38,26	16,00	16.58	265	45	168	6	72	44	H	M	0.5	Giam08
284	FM	1.6	38,26	16,04	14.47	270	56	131	27	31	19	H	L	0.25	Giam08
285	FM	1.2	38,26	16,02	19.33	350	69	116	13	210	16	L	L	0.0625	Giam08
286	FM	1.9	38,26	16,03	19.79	355	69	121	13	215	16	L	L	0.0625	Giam08
287	FM	2	38,27	16,04	13.54	305	51	99	36	199	13	H	L	0.25	Giam08
288	FM	1.7	38,27	16,03	12.5	27	24	125	17	247	60	H	L	0.25	Giam08
289	FM	1.5	38,27	16,02	18.78	221	51	98	24	354	29	H	L	0.25	Giam08
290	F	-	38,27	15,89	-	140	76	351	12	263	8	H	H	1	this work
291	FM	1.1	38,27	16,04	12.48	265	56	126	27	26	19	H	L	0.25	Giam08
292	FM	1.1	38,27	16,04	13.65	17	24	115	17	237	60	H	L	0.25	Giam08
293	FM	1	38,27	16,03	13.22	47	55	287	19	186	28	M	L	0.125	Giam08

294	J	-	38,27	15,23	-	190	84	317	4	47	5	H	M	0.5	this work
295	J	-	38,27	15,90	-	321	85	132	5	222	1	H	M	0.5	this work
296	FM	1.1	38,27	16,04	16.61	27	17	123	17	255	65	H	L	0.25	Giam08
297	FM	1.3	38,27	16,04	12.28	231	64	83	22	348	12	M	L	0.125	Giam08
298	F	-	38,27	15,99	-	132	86	319	4	229	1	H	H	1	Tor95
299	FM	1.5	38,27	16,03	14.58	208	25	117	3	21	65	L	L	0.0625	Giam08
300	FM	1.5	38,27	16,02	16.78	3	14	97	14	230	70	H	L	0.25	Giam08
301	FM	1.5	38,27	16,03	12.56	57	55	297	19	196	28	M	L	0.125	Giam08
302	FM	2.6	38,27	15,03	12.78	172	25	270	17	32	60	H	M	0.5	DeGui13
303	J	-	38,27	15,95	-	234	87	332	0	62	3	H	M	0.5	this work
304	FM	2.1	38,28	16,03	12.04	20	17	118	24	258	60	H	M	0.5	Giam08
305	FM	2	38,28	16,06	19.97	246	60	110	22	12	19	M	L	0.125	Giam08
306	FM	4	38,28	15,17	8.91	180	4	90	4	315	85	H	H	1	Ner05
307	J	-	38,28	15,94	-	184	88	309	1	39	2	H	M	0.5	this work
308	FM	1.9	38,28	16,01	13.24	59	14	149	0	239	76	H	L	0.25	Giam08
309	FM	2.2	38,28	16,03	12.28	242	55	122	19	21	28	H	M	0.5	Giam08
310	FM	2.2	38,28	16,06	19.86	327	78	117	10	208	6	L	M	0.125	Giam08
311	FM	2.6	38,29	15,18	7.8	9	17	108	25	249	60	H	M	0.5	DeGui13
312	FM	2.5	38,29	15,02	14.18	202	42	310	19	58	42	H	M	0.5	DeGui13
313	FM	3.5	38,29	14,97	12.02	207	25	305	17	66	59	H	M	0.5	Scar13
314	FM	2.1	38,29	16,05	16.95	16	11	284	11	150	74	H	M	0.5	Giam08
315	F	-	38,29	15,99	-	143	87	307	2	37	1	M	M	0.25	this work
316	FM	1.7	38,29	16,04	18.49	255	56	116	27	16	19	H	L	0.25	Giam08
317	FM	1.6	38,29	16,00	15.45	241	90	345	0	75	0	M	L	0.125	Giam08
318	FM	2.2	38,29	16,05	18.88	17	47	145	29	252	28	M	M	0.25	Giam08
319	FM	0.9	38,30	16,04	16.04	194	57	64	23	324	23	M	L	0.125	Giam08
320	FM	2.9	38,30	14,99	11.89	173	25	75	17	314	59	H	M	0.5	Scar13
321	J	-	38,31	15,92	-	146	87	329	3	239	0	H	M	0.5	this work
322	FM	0.5	38,31	16,04	18.75	311	42	139	48	45	4	M	L	0.125	Giam08
323	FM	0.8	38,31	16,07	19.63	310	60	130	30	40	0	M	L	0.125	Giam08
324	FM	3	38,32	15,14	28.6	188	19	338	68	95	10	H	M	0.5	Ner05
325	FM	1.2	38,32	16,02	0.01	233	61	77	27	342	10	M	L	0.125	Giam08
326	FM	4	38,32	14,98	4.8	340	68	88	7	228	9	H	H	1	Bill06
327	FM	3.4	38,32	15,03	12.42	174	11	269	23	60	64	H	M	0.5	Scar13
328	FM	3.3	38,33	15,75	14.96	124	57	320	32	225	7	H	M	0.5	Scar13
329	FM	3.4	38,33	14,99	12.18	176	21	268	7	16	68	M	M	0.25	Scar13
330	FM	1.5	38,33	16,09	19.37	310	65	130	25	40	0	M	L	0.125	Giam08
331	FM	1.5	38,33	16,02	11.92	335	47	164	43	69	5	H	L	0.25	Giam08
332	FM	4.1	38,33	14,90	11.04	187	27	293	27	60	50	H	H	1	Scar13
333	FM	0.8	38,33	16,10	19.53	295	42	168	33	56	30	L	L	0.0625	Giam08
334	FM	3.5	38,33	14,89	10.01	214	82	88	5	357	6	M	M	0.25	Scar13
335	FM	1.2	38,33	16,09	19.51	295	42	168	33	56	30	L	L	0.0625	Giam08
336	FM	0.7	38,33	16,10	19.05	305	60	125	30	35	0	H	L	0.25	Giam08
337	FM	1	38,33	16,09	19.45	315	65	135	25	45	0	M	L	0.125	Giam08

338	FM	2.7	38,33	14,89	8.62	358	38	268	1	177	52	M	M	0.25	Scar13
339	FM	1.1	38,33	16,09	19.15	234	48	70	38	334	8	L	L	0.0625	Giam08
340	FM	1.5	38,33	16,09	19.11	259	64	103	24	9	9	M	L	0.125	Giam08
341	FM	1.6	38,33	16,09	19.78	305	60	125	30	35	0	H	L	0.25	Giam08
342	FM	0.6	38,33	16,10	19.08	341	64	137	24	231	9	H	L	0.25	Giam08
343	FM	1.6	38,33	16,09	19.65	305	60	125	30	35	0	H	L	0.25	Giam08
344	FM	3.2	38,33	14,88	12.01	307	0	41	83	217	7	L	M	0.125	Scar13
345	FM	1.7	38,34	16,14	19.73	310	74	84	11	176	11	H	L	0.25	Giam08
346	FM	1.2	38,34	15,95	20.72	92	52	348	11	250	36	H	L	0.25	Giam08
347	FM	2.8	38,34	14,91	11.33	354	0	264	14	84	76	H	M	0.5	Scar13
348	FM	1.9	38,34	16,12	17.11	26	68	151	13	245	17	H	L	0.25	Giam08
349	FM	1.5	38,34	15,94	17.41	159	32	63	9	319	56	H	L	0.25	Giam08
350	FM	1.4	38,34	15,94	17.36	179	28	88	1	356	62	H	L	0.25	Giam08
351	FM	1.3	38,34	15,94	17.82	181	38	79	15	332	48	H	L	0.25	Giam08
352	FM	2	38,34	15,94	16.46	166	28	69	13	317	59	M	L	0.125	Giam08
353	FM	2.1	38,34	15,94	16.49	161	31	56	23	296	50	H	M	0.5	Giam08
354	FM	1.4	38,34	15,94	16.41	166	28	69	13	317	59	H	L	0.25	Giam08
355	FM	1.9	38,34	15,94	16.53	155	45	335	45	65	0	H	L	0.25	Giam08
356	FM	4.1	38,35	14,90	12.34	0	19	252	42	108	42	H	H	1	Scar13
357	FM	3.5	38,35	14,88	13.79	153	6	247	36	55	53	H	M	0.5	Scar13
358	FM	1.6	38,35	16,07	16.95	259	64	103	24	9	9	L	L	0.0625	Giam08
359	FM	1.3	38,35	15,95	15.78	157	41	344	49	250	4	H	L	0.25	Giam08
360	FM	3	38,35	15,94	18.55	113	44	17	7	280	45	L	M	0.125	Giam08
361	FM	4.8	38,35	14,89	13.46	153	36	247	6	345	53	H	H	1	Scar13
362	FM	3.8	38,36	14,87	13.4	342	15	248	15	115	69	H	M	0.5	Scar13
363	FM	2.9	38,36	14,89	12.84	174	3	265	11	69	79	H	M	0.5	Scar13
364	FM	2.7	38,36	15,04	10.7	308	15	187	63	44	22	H	M	0.5	Scar13
365	FM	3.4	38,36	14,82	14.4	12	4	279	32	108	58	H	M	0.5	Scar13
366	FM	3	38,36	15,78	16.55	188	76	284	1	14	14	H	M	0.5	Scar13
367	FM	3.7	38,36	14,88	11.38	173	25	75	17	314	60	M	M	0.25	Ner05
368	FM	1.1	38,37	16,14	15.37	272	55	172	7	77	34	H	L	0.25	Giam08
369	FM	1.9	38,37	16,09	11.14	210	11	119	3	14	79	H	L	0.25	Giam08
370	FM	1.4	38,37	15,99	13.43	306	41	145	48	44	10	M	L	0.125	Giam08
371	FM	1.3	38,38	16,14	14.76	82	38	234	48	341	14	H	L	0.25	Giam08
372	FM	2.2	38,38	16,17	16.06	210	40	314	16	61	46	H	M	0.5	Giam08
373	FM	2.5	38,39	16,14	11.97	355	53	257	6	162	36	M	M	0.25	Giam08
374	FM	5.5	38,39	15,07	14,00	355	23	93	18	217	60	H	H	1	Pre13
375	FM	1.5	38,40	16,14	17.67	347	48	122	33	228	23	H	L	0.25	Giam08
376	FM	2	38,41	16,14	17.7	301	64	97	24	191	9	H	L	0.25	Giam08
377	FM	1.1	38,41	16,14	18.46	333	52	110	29	213	22	M	L	0.125	Giam08
378	FM	1.7	38,41	16,14	18.28	231	38	129	15	22	48	M	L	0.125	Giam08
379	FM	2.7	38,42	14,93	9.76	141	74	274	11	6	11	H	M	0.5	Scar13
380	FM	1.1	38,42	16,16	17.07	324	64	95	18	191	18	H	L	0.25	Giam08
381	FM	2.8	38,43	15,82	13.6	97	70	192	2	283	20	H	M	0.5	Pre13

382	FM	1.7	38,43	16,15	9.12	250	70	70	20	340	0	L	L	0.0625	Giam08
383	FM	1.9	38,43	15,94	16.42	279	33	23	21	140	49	L	L	0.0625	Giam08
384	FM	1.8	38,44	15,97	16.08	87	55	342	10	245	33	H	L	0.25	Giam08
385	FM	2.9	38,44	15,08	10.26	172	7	272	56	77	33	H	M	0.5	Scar13
386	FM	1	38,44	15,92	12.98	140	60	320	30	50	0	L	L	0.0625	Giam08
387	FM	2	38,44	16,20	21.06	265	69	73	20	165	4	L	L	0.0625	Giam08
388	FM	2.4	38,44	16,07	20.96	176	64	28	22	293	12	H	M	0.5	Giam08
389	FM	2.5	38,45	14,94	5.31	230	45	50	45	140	0	H	M	0.5	Ner05
390	FM	4.2	38,45	15,10	8.84	111	22	341	57	211	23	H	H	1	Scar13
391	F	-	38,45	16,12	-	273	53	94	36	3	1	H	M	0.5	this work
392	FM	4.6	38,45	15,10	11.12	112	22	324	65	207	12	H	H	1	Scar13
393	FM	2	38,45	16,11	14.21	188	24	311	51	84	29	H	L	0.25	Giam08
394	FM	3	38,46	16,04	9.51	174	9	270	32	70	56	H	M	0.5	Scar13
395	FM	1.1	38,47	16,15	24.52	344	60	120	22	218	19	H	L	0.25	Giam08
396	FM	2.3	38,47	15,95	13.59	197	42	297	11	39	46	H	M	0.5	Giam08
397	FM	1.6	38,47	16,15	20,00	316	55	104	31	203	15	H	L	0.25	Giam08
398	FM	1.6	38,48	16,02	16.04	108	71	320	16	227	10	H	L	0.25	Giam08
399	J	-	38,48	16,04	-	265	48	174	1	84	42	H	M	0.5	this work
400	FM	1.4	38,48	16,05	21.73	118	60	335	24	238	16	H	L	0.25	Giam08
401	FM	3.2	38,48	15,10	11.2	146	20	34	45	253	38	M	M	0.25	Ner05
402	FM	2.7	38,49	14,80	17.14	316	10	221	25	66	63	M	M	0.25	Scar13
403	FM	1.9	38,49	16,02	22.12	125	48	324	41	226	10	H	L	0.25	Giam08
404	FM	1.6	38,49	16,02	21.92	94	48	302	38	201	14	L	L	0.0625	Giam08
405	FM	1.6	38,49	16,02	22.53	61	31	316	23	196	50	L	L	0.0625	Giam08
406	FM	2.1	38,49	16,03	21.73	94	48	302	38	201	14	L	M	0.125	Giam08
407	FM	1.9	38,49	16,02	21.93	94	48	302	38	201	14	L	L	0.0625	Giam08
408	FM	1.5	38,49	16,03	21.61	105	48	304	41	206	10	L	L	0.0625	Giam08
409	FM	2	38,49	16,02	21.89	124	48	332	38	231	14	H	L	0.25	Giam08
410	FM	2.1	38,49	16,02	22.23	124	48	332	38	231	14	H	M	0.5	Giam08
411	FM	1.1	38,49	16,02	22.16	140	47	329	42	235	5	L	L	0.0625	Giam08
412	FM	1.9	38,49	16,02	21.37	162	65	333	25	65	3	H	L	0.25	Giam08
413	FM	1.2	38,49	16,03	22.01	94	48	302	38	201	14	L	L	0.0625	Giam08
414	FM	1.3	38,49	16,03	21.41	105	48	304	41	206	10	L	L	0.0625	Giam08
415	FM	2	38,49	16,02	21.35	203	25	112	3	16	65	M	L	0.125	Giam08
416	FM	1.8	38,49	16,02	21.71	73	52	288	33	186	17	M	L	0.125	Giam08
417	FM	1.6	38,49	16,03	21.94	171	54	358	36	266	3	L	L	0.0625	Giam08
418	FM	3.2	38,49	14,84	12.51	310	36	71	35	190	35	H	M	0.5	Scar13
419	FM	3.7	38,51	14,81	16.4	329	10	64	25	219	63	H	M	0.5	Scar13
420	J	-	38,51	16,05	-	245	71	76	19	345	3	M	M	0.25	this work
421	J	-	38,51	16,05	-	289	62	77	25	173	13	H	M	0.5	this work
422	FM	3.1	38,51	14,83	7.38	147	11	46	42	249	46	H	M	0.5	Scar13
423	J	-	38,51	16,09	-	345	89	166	1	76	0	H	M	0.5	this work
424	J	-	38,53	16,06	-	329	87	133	3	223	1	H	M	0.5	this work
425	FM	1.4	38,53	15,94	21.16	116	67	320	21	227	9	H	L	0.25	Giam08

426	FM	3.5	38,53	15,93	15,00	26	58	153	21	253	23	H	M	0.5	Pre13
427	FM	2.9	38,53	14,80	15.5	143	11	37	52	240	36	M	M	0.25	Ner05
428	J	-	38,53	16,03	-	185	88	67	1	337	2	H	M	0.5	this work
429	FM	2.1	38,54	16,05	17.35	115	69	349	13	255	16	H	M	0.5	Giam08
430	FM	1.4	38,54	16,05	24.76	74	69	334	4	243	31	M	L	0.125	Giam08
431	F	-	38,55	15,94	-	182	74	347	15	78	4	H	H	1	Ghi79a
432	F	-	38,56	16,19	-	26	86	165	3	255	2	H	M	0.5	this work
433	FM	2	38,57	16,03	21.49	81	41	321	31	207	34	H	L	0.25	Giam08
434	J	-	38,58	16,21	-	21	2	290	48	113	42	L	M	0.125	Ghi79a
435	FM	3.1	38,59	14,80	6,00	23	1	292	23	115	67	H	M	0.5	Pre13
436	FM	1.7	38,59	16,01	20.94	38	59	154	15	252	27	L	L	0.0625	Giam08
437	F	-	38,61	16,23	-	90	83	284	7	194	2	H	H	1	Ghi79a
438	F	-	38,62	16,25	-	261	77	38	8	123	9	H	M	0.5	this work
439	F	-	38,68	16,13	-	124	78	290	11	20	3	H	M	0.5	this work
440	F	-	38,70	16,15	-	296	83	44	2	134	7	H	M	0.5	this work